



Manfred Stamm

Contents

1	Introduction	348
2	Specific Aspects of Polymer Surfaces	352
2.1	Chain Conformation	352
2.2	Surface and Interfacial Tension	357
2.3	Functional Polymer Surfaces	360
3	Interfaces in Blends, Copolymers, and Composites	367
3.1	Interfaces Between Homopolymers	368
4	Characterization Techniques of Polymer Surfaces and Interfaces	375
4.1	Surface and Interfacial Tension	378
4.2	Scanning Force Microscopy (SFM)	378
4.3	Ellipsometry (ELLI) and Surface Plasmon Spectroscopy (SP)	379
4.4	Scanning and Transmission Electron Microscopy (SEM, TEM)	379
4.5	X-Ray Photoelectron Spectroscopy (XPS)	380
4.6	Electrokinetic Methods (Zeta Potential)	381
4.7	Infrared Spectroscopy (ATR-FTIR)	381
4.8	Raman Spectroscopy	381
4.9	X-Ray and Neutron Reflectometry (XR, NR, GISAXS)	382
4.10	Secondary Ion Mass Spectrometry (SIMS)	383
4.11	Ion Techniques	383
4.12	Optical Microscopy Techniques (OM)	384
4.13	Indentation, Adhesion, Mechanical Properties	384
4.14	Inverse Gas Chromatography (IGC)	385
5	Summary and Outlook	386
	References	386

M. Stamm (✉)

Institute of Physical Chemistry and Physics of Polymers, Leibniz-Institut für Polymerforschung
Dresden e. V., Dresden, Germany
e-mail: stamm@ipfdd.de

Abstract

Polymer surfaces and interfaces are present with all polymer materials. They determine many properties like optical appearance, wetting, and adhesion, but with blends and composites also for instance toughness, hardness, modulus, and elongation at break. A short outline of polymer surfaces at molecular scale is given with reference to special aspects of chain conformation and surface dynamics. The surface tension as a fundamental property of a surface is discussed and surface functionalization in particular by grafting of polymer brushes onto surfaces described. In this way, a very versatile surface functionalization and even responsive polymer brush surfaces can be obtained. They may be used to control wetting, adhesion, bio-functionality, catalytic activity, and sensing ability. The interface between polymers can be formulated on the basis of mean-field theory with introduction of an effective interaction parameter, which is related with interface width and fluctuations at the interface. Polymer blends, copolymers as compatibilizers, and composites are discussed as examples, where interfaces play an essential role. Several techniques for surface and interface characterization including scanning force and electron microscopy, photoelectron and IR/Raman spectroscopy, as well as x-ray and neutron reflectometry or scattering techniques are critically reviewed. Guidelines for resolution and typical information obtained are provided. The importance of surface and interface design for future high-tech devices and advanced materials is highlighted.

Keywords

Surfaces · Interfaces · Wetting · Blends · Copolymers · Composites · Functionalization · Brushes · Analysis · Characterization · Surface tension · Contact angle · Electron microscopy · X-ray scattering · Neutron scattering · Reflectometry · Scanning force microscopy · XPS · SIMS · Ion beam techniques

1 Introduction

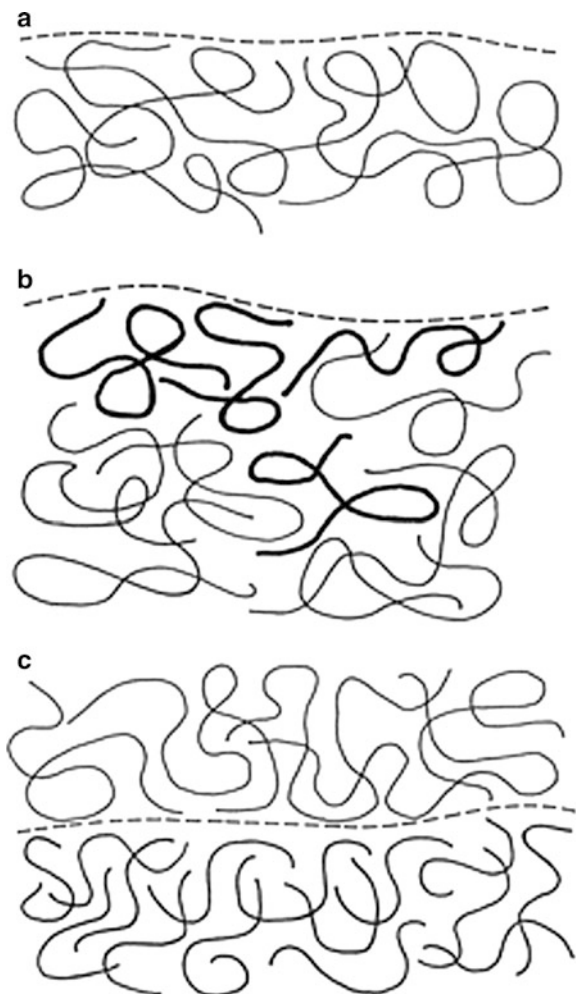
The surfaces and interfaces of polymers are important for many properties of polymeric materials, and their design can introduce interesting functionalities. This is for instance true for polymer blends, where the interface between incompatible polymers strongly influences the mechanical properties, or for the application of lightweight composite materials in cars or airplanes, where adhesion between the reinforcing fibers and the soft polymer matrix plays an essential role. Very special properties can be achieved with polymer nanocomposites, where functional nanoparticles are dispersed in a polymer matrix or with thin smart polymer brush layers as coatings on surfaces, which allow control of wetting and adhesion properties. Looking on everyday polymeric parts in household, cars, or sports, one could ask questions like “how do they feel” or “how do they look,” which in many cases will critically influence the decision for the purchase of a product. The appearance depends on “the surface,” and the optical or mechanical properties but also corrosion or scratch resistance depend largely on surface

composition and structure. A thin functional layer at the surface can influence those properties significantly. This is in particular the case, when even functional or smart surfaces or interfaces are used, which can provide biocompatibility, switching or adaptive properties. The characterization of polymer surfaces and interfaces in many cases requires special or adapted techniques, and often only a combination of different techniques will provide necessary information. A careful characterization is however the prerequisite for the understanding and dedicated design of materials properties [1, 2].

One should be aware of the fact that one may understand quite different aspects when talking about polymer surfaces and interfaces. Depending on the properties under consideration, the surface or interfacial region may extend from subnanometers to micro- or even millimeters, which covers a range of more than 6 orders of magnitude [1–10]. If one is looking at individual polymer chains (Fig. 1), the surface and interfacial region will typically range over one chain, where a measure of the chain size, the radius of gyration, is of the order of 3–30 nm depending on molecular weight. On the other hand, very different microscopic properties or in general a combination of them could be important to achieve a particular surface macroscopic property or appearance. So for instance, for the wetting of a smooth surface by a liquid, the composition of the outermost surface layer will be important for the wetting behavior and one has to consider the composition of the first atomic layer even at subnanometer scale. When on the other hand the optical properties of a surface are important, one is dealing with a surface layer in the range of the wavelength of light, that is typically several hundred nanometers large, while for the adhesion between two sheets of polymeric materials a plastic deformation region in the vicinity of the interface of up to millimeters may be important because a large part of the deformation energy is dissipated in this plastic zone. Thus, different applications require different approaches with respect to desired surface or interface modifications as well as the use of different characterization techniques, and one needs a careful definition of the problem before looking for details of surfaces and interfaces.

A compilation of some common surface and interface analysis techniques is presented in Tables 1 and 2 indicating typical information that can be obtained utilizing a particular technique as well as its typical minimal information depth. With most techniques, the sample preparation and proper adoption of the technique is of particular importance. The parameters indicated will in most cases depend on the mode used, the sample system, the available contrast, the addition of, e.g., fluorescent dyes, and some quantities cannot be obtained completely independent from each other. Thus for instance, there exist several different optical microscopy techniques ranging from simple dark and bright field to differential interference, fluorescent, or phase measurement interference techniques. For those different optical microscopy techniques, the available information is quite different from each other. This is similarly true for scanning force microscopy, electron microscopy, etc., where always techniques are improved, extended, and further developed. So these tables can only be seen as a rough guide for selection of particular techniques and of course are far from being complete.

Fig. 1 Schematics of polymer surfaces and interfaces, (a) homopolymer surface, (b) blend surface with surface enrichment of one component, and (c) interface between polymers with no interdiffusion. (From Ref. [3])



There are plenty of reviews and books available which cover polymer surfaces and interfaces (see [1, 2, 4, 5]) as well as particular aspects and characterization (see [3, 6–11]). In the following, we cover briefly some basic aspects of polymer surfaces and interfaces including some ways for particular functionalization and shortly outline some important analytical techniques from Tables 1 and 2.

We distinguish in Tables 1 and 2 between surface and interface analysis techniques, while this distinction is not rigorously true [3]. So several techniques are applicable for both surface and interface analysis (e.g., x-ray reflectometry, SIMS, optical techniques, etc.), when they are used in different modes of application. Also the optimal sample requirements are different from one technique to the next, and the surface might be facing air, liquid, vacuum, or even a polymer solution. For a particular technique, the choice and the information content will depend of course very much on this environment, and therefore one has to be very careful, to analyze

Table 1 Most common techniques for surface characterization

Technique	Probe in/out	Smallest information depth/width lateraly (nm)	Information	Comments
Surface tension/ contact angle ST	Liquid drop	0.1/–	Surface energy	Easy to use, molecular information difficult
Scanning force microscopy SFM	Cantilever	0.05/1	Surface topography, composition, toughness etc.	Atomic resolution. Many different modes
Ellipsometry ELLI	Polarized light	0.1/300	Thin surface layer	Molecular interpretation difficult
Scanning electron microscopy SEM	Electrons	1/1	Surface topography	Vacuum technique
X-ray photoelectron spectroscopy XPS	X-rays/ electrons	5/2000	Chemical composition, binding state	Quantitative, vacuum technique, lateral imaging possible
Electrokinetic measurements/ zeta potential	Voltage	0.1/–	Surface charge	Measurement in aqueous medium
Infrared attenuated total reflection ATR-FTIR	Infrared light	2000/2000	Surface composition, binding state	Specific ATR-crystal needed
Raman spectroscopy/ microscopy RS (resonance enhanced)	Light	0.5/300	Surface composition, binding state	Resonance enhancement with metal clusters
X-ray reflectometry XR Grazing incidence x-ray small angle scattering GISAX	X-rays	0.5/2000 0.5/0.1	Surface roughness, thin surface layers, lateral structure	Flat surfaces required
Focused ion beam FIB	Ions (electrons)	2/10 (1 with SEM)	Imaging, cutting, deposition	Nanomanipulation possible, often in combination with SEM
Scanning tunneling microscopy STM	Cantilever	0.05/1	Tunneling current	Surface conductivity required
Optical microscopy/ interferometry OM	Light	0.1/300	Surface roughness, structure	Many possibilities, good height resolution with interference techniques
Surface plasmon spectroscopy SP	Light/ plasmons	0.1/300	Thin surface layers	Metallic layer on prism necessary

(continued)

Table 1 (continued)

Technique	Probe in/out	Smallest information depth/width laterally (nm)	Information	Comments
Secondary ion mass spectroscopy SIMS	Ions	0.1/1000	Surface composition, contaminations	“Static” mode, vacuum technique
Micro-indentation MI	Cantilever	100/200	Surface hardness, module	Quantitative interpretation difficult
Neutron reflectometry NR	Neutrons	0.5/2000	Surface roughness, enrichment layer	Deuterated compounds needed
Auger spectroscopy AS High-resolution electron energy loss spectroscopy HREELS	Electrons	0.2/100 1	Electronic excitation, surface composition Vibration spectrum	Surface conductivity needed Vacuum technique
Scanning near field optical microscopy SNOM	Light	1/50	Vibrational modes, fluorescence, orientation	Local optical spectroscopy possible
Inverse gas chromatography IGC	Gas	0.1/–	Gas adsorption, surface functionality, energetics	Measurement on powder

the true materials behavior and not artifacts. On the other hand, one could also just be interested in a thin contamination layer at the surface, which can change surface appearance of materials quite significantly. Also resolution does depend on many parameters and is sensitive in particular on sample conditions and on preparation, so only “typical” values for favorable conditions are given in the tables. With those comments, one should be aware that in this short review not all aspects of polymer surfaces and interfaces can be discussed, and many techniques have elegant ways to focus on particular aspects and can overcome some of their shortages.

2 Specific Aspects of Polymer Surfaces

2.1 Chain Conformation

Polymers are very long molecules with specific properties, which are determined by conformational aspects as well as by chemistry given by the constitution of monomers. The architecture of the molecules, i.e., linear, branched, crosslinked, or even

Table 2 Most common techniques for interface characterization

Technique	Probe in/out	Typical smallest information depth (nm)	Typical information	Comments
Pendent drop	Liquid	0.2	Interface tension	Indirect technique
Transmission electron microscopy TEM	Electrons	0.5	Absorption/reflection of electrons, interface width	Cut perpendicular to interface, staining
Focused ion beam FIB	Ions (electrons)	10 (1 with SEM)	Concentration profile, element distribution, interface width	Cut perpendicular to interface with ions, imaging with SEM
X-ray reflectometry XR	X-rays	0.2	Interference fringes, interface width/roughness	Contrast of heavy elements
Secondary ion mass spectrometry dynamic SIMS	Ions	20	Element distribution, interface width	Dynamic (destructive) technique
Neutron reflectometry NR	Neutrons	0.2	Interference fringes, interface width/roughness	Contrast by deuteration
Scanning force microscopy SFM	Cantilever	0.2	Interface width/roughness/topography	Cut perpendicular to interface/etching, dissolution/hard tapping
Elastic recoil detection ERD Forward recoil spectroscopy FRD	$^4\text{He}/^1\text{H}$, ^2H (H, D)	20	H/D distribution, interface width	Contrast by deuteration
Nuclear reaction analysis NRA	$^{15}\text{N}/\gamma$ (4.4 MeV) $^3\text{He}/^4\text{He}$	12	H/D distribution, interface width	Contrast by deuteration
Rutherford backscattering RBS	$^4\text{He}/^4\text{He}$	30	Backscattering from heavy atoms, interface width	Contrast from heavy atoms
Small angle x-ray scattering SAXS	X-rays	1	Porod analysis, electron density variation, interface width	Bulk sample possible
Nuclear magnetic resonance NMR	Magnetic field	1	Spin diffusion from species, interface width	Bulk sample possible
Fluorescence quenching	Light	0.3	Quenching of donor/acceptor molecules	Fluorescence tagging of molecules necessary

star-like or H-shaped, plays a major role on the properties. At the surface, chain conformations are specific, and various chemical surface modifications are possible. So the surface properties can be largely modified by surface functionalization caused for instance by surface enrichment of components, adsorption, or grafting of chains at the surface or coating of a thin film. In that way, surface properties can be tuned independently from bulk properties, and also switching of surface properties is possible. Those aspects are addressed below, and we first discuss some basic properties of linear homopolymers at surfaces connected with chain conformations, topography, and structure. Because of the wealth of possibilities, we will concentrate on homopolymer surfaces, while many of the polymer surface topics are covered by books and reviews [1–11].

A long, flexible polymer chain possesses a huge number of internal degrees of freedom which is the origin of conformational entropy [10, 12–14]. This property related with the length of polymer chains is the key for the understanding of polymer behavior and distinguishes polymers from small and stiff molecules. It leads to unique properties also at surfaces. The simplest model for a flexible polymer molecule in melt, glassy state and in solution is the Gaussian chain. The chain is artificially subdivided into segments, whose directions are uncorrelated in space. These segments, so-called statistical or Kuhn segments, typically consist of several chemical repeat units of the real chain. The size of the segments corresponds to the persistence length of the chain, i.e., the distance over which orientation correlations between monomers decay. Chemical details of the original chain are mapped into the actual length of the statistical segment and into (effective) interaction parameters between pairs of such segments. For instance, the statistical segment length of polyethylene corresponds to about 5 CH₂ units which is about half a nanometer.

The size of a polymer chain is characterized by the average distance between the chain ends R or the radius of gyration R_g (average distances of segments from the center of mass of the chain). For an ideal chain we have.

$$\langle R^2 \rangle = a^2 N = 6 \langle R_g^2 \rangle \quad (1)$$

Here, a denotes the statistical segment length and N the number of segments (repeat units). The brackets indicate the statistical average. It is obvious that the size of the (statistical) coil formed by a polymer chain is much smaller than its contour length: $R \ll Na$. Typically, the size of synthetic polymer chains is in the range between a few nanometers up to some tens of nanometers. Long stiff biological polymers such as DNA can have a size in the range of several micrometers.

To discuss specific properties of polymer chains in solution at solid surfaces, we have to distinguish the cases, here the surface has attractive (absorbent) or repulsive character with respect to the monomers. Free surfaces, i.e., surfaces formed against air (or vacuum) are considered as a special class of repulsive surfaces where the surface tension of the polymers is the characteristic property. If we consider a chain close to a surface, its conformational degrees of freedom are reduced by the geometrical constraints and so is the chain entropy.

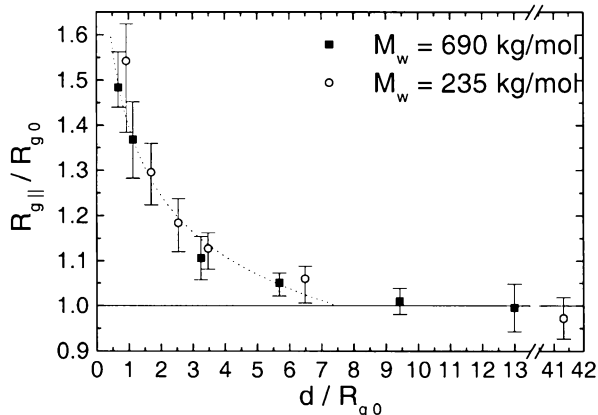
In order to keep a polymer chain in a *dilute solution* close to the surface, an energetic compensation is necessary. This leads to a phase transition scenario for attractive surfaces: Above a critical temperature of adsorption T_c or below a critical adsorption strength of the surface, the polymer chains avoid the surface and form a depletion zone, while below T_c , polymer chains are adsorbed and conformations change into “pancake-like,” quasi two-dimensional shape [15–17]. This is in particular true if individual chains are adsorbed on a flat surface from highly diluted solution. In case of strong adsorption at a flat surface, the chain conformation in the adsorbed state can be directly measured by atomic force microscopy [17]. Under special conditions, it is expected that the adsorbed chain conformations reflect the ones in solution which allows the direct visualization of those chain conformations. In this way, for instance, conformational phase transition in polyelectrolytes can be followed in detail [18].

When the bulk phase is dense (*melt, glassy state*), the layer close to the surface is densely filled independently on substrate interactions. In computer simulations, evidence can be found for changes of chain conformations in the vicinity of the free surface at a scale related to R_g but also deviations on smaller length scales. This includes an enrichment of chain ends at the surface [20] and a flattened chain conformation in direct vicinity at the surface [19]. However, the contribution of chain ends to the free energy and surface tension is rather weak (neglecting chemical effects), typically of the order $1/N$. Despite the problem of free energy and surface tension, a solid surface influences the chain conformations in other subtle ways. This regards the interpenetration or entanglements between the chains close to the surface [22]. As a consequence of neutral boundary conditions, the chain volume is squeezed if chains are located close to the surface. Therefore, the number of other chains penetrating the volume of a chain close to the surface is reduced. Conservation of monomer number (dense melt) leads to a reduction of entanglements by a factor of $1/2$ for long chains close to the surface. Since entanglement properties are essential material properties which determine dynamic properties of polymers, this effect can be important. Experiments give indication for such a reduction of the entanglement density [23]. Generally, it is difficult to observe individual chain conformations close to the surfaces experimentally, but some experiments are available in thin films. From neutron scattering experiments, where the radius of gyration is measured in very thin films, it is concluded that the chain conformation in confined dimensions flattens and R_g changes as much as 50% [19, 24] (Fig. 2).

One has to take into account that neutron scattering averages laterally over a certain region. Taking those effects into account, one can conclude that surface effects on the conformation extend over several R_g . So there is a quite good agreement between experiment and theory. In that range, also entanglement effects are expected (but not directly measured), where entanglements should be reduced in the vicinity of the free surface.

As a trivial effect, there is however also a surface tension connected with capillary waves at polymer melt surfaces. In comparison to low-molecular-weight samples, the capillary waves depend not only on surface tension and temperature but also on viscoelasticity [16] and reflect entanglement effects [25]. With polymers, the surface

Fig. 2 Measurement of the radius of gyration by small-angle neutron scattering SANS in thin films of polystyrene of different molecular weights. When the film thickness d approaches $6R_{g0}$, the flattening of the chains is observed. R_{g0} is the radius of gyration in the bulk film, while $R_{g\parallel}$ denotes the radius of gyration in the plane of the film measured in the experiment. (Data from Ref. [19])



structures are however in many cases not at equilibrium, but frozen-in into the glassy state from preparation. Upon heating, one then can observe formation of surface roughness due to development of capillary waves at larger scales as well as smoothing at small length scales [26, 27].

The presence of an interface or a solid surface influences also dynamical processes. Since reptation requires strong interpenetration of chains, close to a surface reptation dynamics should be accelerated. However, it is rather difficult to measure dynamical effects in the surface region (some nm above the surface only). Computer simulations gave first indications for surface effects on entanglement properties [28]. Polymers below the glass-transition temperature T_g display solid-state mechanical properties. Here, fluctuations are frozen on larger time scales. The temperature T_g is specific for each polymer. With the growing interest in thin polymer films, also measurements of the glass-transition temperature has been carried out for polymers under various geometrical constraints (thin films, pores, with or without substrate). The results obtained are controversial. Based on the previous discussion of dynamics in polymer melts, one might expect a higher mobility of polymer chains close to the surface and thus a decrease of T_g . In fact, such results have been reported experimentally for free-standing polystyrene films where a reduction of T_g of about 70 K has been observed [67]. Other authors found a strong dependence of the substrate/polymer interaction on the change of T_g [29] and reported an increase of T_g close to the surface. Part of the controversy may be due to the fact that different experimental methods and sample preparation techniques are used in different publications. There are recent results that surface effects on dynamics are only minor [30]. Also from neutron reflectivity experiments, one can conclude that chain dynamics is only influenced in a region of the order of R_g [31] (Fig. 3). In this case, the interdiffusion between two films is measured at a temperature close to T_g , where the thickness of one film is varied from $d = 0.3$ to $4.6 R_g$. The interdiffusion is sensitive on the region close to the surface, where a slight increase of dynamics at film thicknesses smaller than R_g is observed. This is reflected by an increased interdiffusion width σ at given interdiffusion time τ_d between two films, where one film has thickness smaller than R_g .

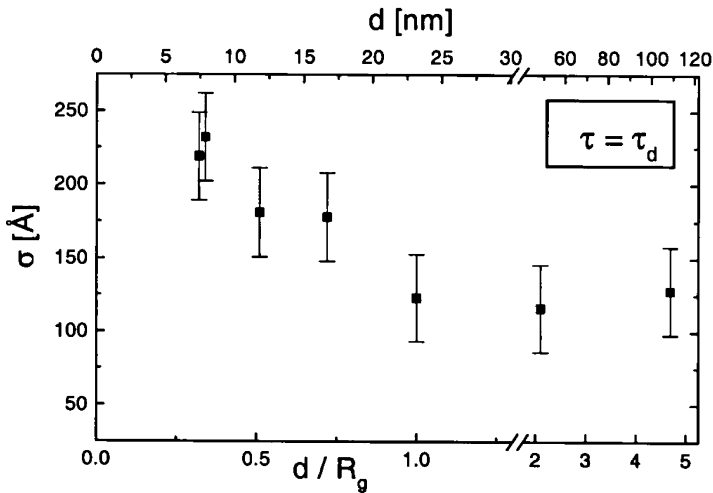


Fig. 3 Determination of chain mobility in thin films of thickness d via neutron reflectometry. The interdiffusion width σ after interdiffusion of time τ equal to disentanglement time τ_d is determined for polystyrene films as function of film thickness d . (From Ref. [31])

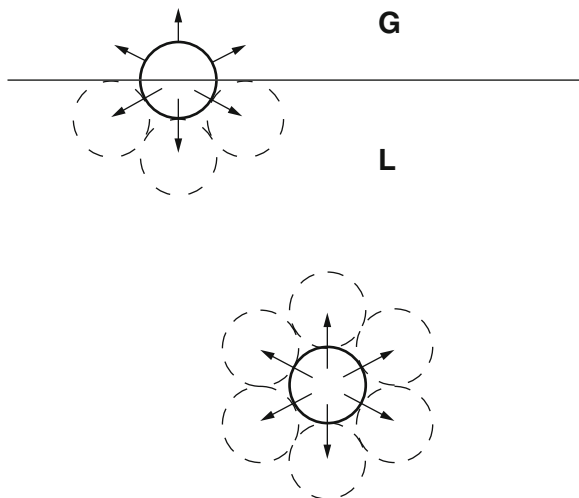
This could be attributed to effects of entanglements, which are expected to be reduced close to the surface, and chain ends, which should be enriched at the surface. One therefore can conclude that surface effects on chain conformation and chain dynamics are restricted to a region of the order of R_g .

2.2 Surface and Interfacial Tension

The most common way to obtain a picture of the surface properties [3, 8, 9, 11, 32, 33] and to measure the surface energetic state is the determination of the *surface tension*. It is determined by the outermost layers of atoms and therefore by a surface region of typically 0.2 nm. It arises from the asymmetric surrounding of atoms at the surface, where an atom at the surface is missing some of its neighboring atoms and consequently experiences a force due to the remaining asymmetric interactions (Fig. 4).

The surface tension turns out to be a very fundamental property of solids and liquids [3, 8], since it reflects directly the strength of the bonding within the bulk material which is schematically shown in Fig. 4. There are very different binding forces, and hard solids (covalent, ionic, metallic) typically reveal “high-energy” surfaces (surface tension ~ 500 to 5000 mJ/m²), which is in contrast to weak molecular solids and liquids (soft matter) with their “low-energy” surfaces (surface tension < 100 mJ/m²). It is clear that most polymers belong to the second class of materials and interactions between the chains are dominated typically by van der Waals forces, and in some cases by hydrogen bonds. Surface tension however also depends on surface roughness and will be influenced by surface segregation of

Fig. 4 Schematics of a molecule in bulk (liquid) and at the surface (interface liquid/gas) showing neighboring molecules and interaction forces [33]



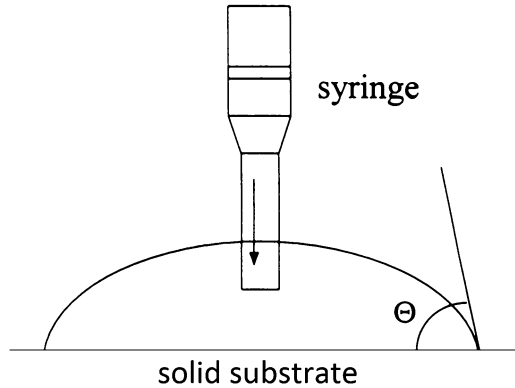
components (surfactants, antioxidants, etc.) and in particular by contaminations (catalyst, solvent, etc.). Therefore, in many practical cases, it may not reflect the properties of bulk material but of a thin surface layer or even end groups which may also segregate to the surface. Using surface tension measurements provides information on surface composition and structure only in a very indirect way, while it is relatively easy to measure in the lab and may provide helpful practical information for application.

In applications, surface and interfacial tensions of polymers are quite important such as in wetting and coating processes, in blending of polymers, in biocompatibility, and in adsorption and corrosion processes. The adhesion, and friction as well as behavior of colloidal dispersions (paints, cosmetics, etc.) are influenced by surface and interface tension. The interrelationships between interfacial aspects and materials properties are despite of their importance still poorly understood. The measurement of surface tensions of polymers is usually performed by determination of the *contact angle*, where a liquid drop is positioned on the sample surface. The equilibrium contact angle Θ for such a drop on a homogeneous smooth surface depends on corresponding interfacial tensions as expressed by the Young equation [8, 32]:

$$\gamma_{LV} \cos \Theta = \gamma_{SV} - \gamma_{SL} \quad (2)$$

γ_{LV} denotes the surface tension of the liquid with its saturated vapor, γ_{SV} the surface tension of the solid with the saturated vapor, and γ_{SL} the interfacial tension between solid and liquid. It is a consequence of the equilibrium of interfacial forces at the three-phase boundary at the edge of the drop. While the contact angle between drop and sample surface is typically measured at the drop edge, also drop profile analysis techniques may be used which enhance the sensitivity. The drop volume can be continuously enlarged (advancing contact angle) or decreased (receding contact angle), and measurements may be performed in a dynamic way. For inhomogeneous

Fig. 5 Scheme of contact angle measurement. A drop is put on a solid substrate via a syringe and the contact angle Θ at the edge of the drop is measured



and rough surfaces, one often observes that the advancing and receding contact angles are significantly different from each other. Dynamic measurements are performed with the goniometer sessile drop technique where the drop is deposited on the surface by a motor-driven syringe, and the volume is increased or decreased at given speed to measure dynamic advancing and receding contact angles (Fig. 5).

With the so-called ADSA technique (axisymmetric drop shape analysis), a silicon wafer with a small hole is used where the polymer to be investigated is deposited as a thin film [3]. From below the wafer, the liquid is put via the hole onto the wafer with a motor-driven syringe at constant speed and the increasing drop is monitored by a video camera. By computer analysis of the drop profile, the advancing contact angle is determined. Then the volume of the drop is decreased at constant speed via the syringe, and the receding contact angle is determined. Those contact angles will in general depend on the speed and possibly reach after some initial time a constant value, but in most cases advancing and receding contact angles are different from each other. For ideal surfaces, they should coincide. One has to be in particular careful to avoid influence of surface contaminations like antioxidants, catalyst, etc., which may be enriched at the surface and where already small amounts can influence the contact angle significantly. Also the liquid used (in most cases water) has to be inert to the surface material. If the surface interacts or swells with the liquid, one can use the captive air bubble technique, where in an inverted setup, the surface is constantly covered with the liquid and the syringe introduces from the top an air bubble via a small hole in the silicon wafer. There are several other techniques used (e.g., Wilhelmy balance technique with a plate or capillary penetration/Washborn technique with a powder) and several types of commercial instruments are available to measure contact angles accurately. If disperse and polar contributions to surface tension are obtained from measurements with several liquids of different polarity, the free surface energy can be calculated [8].

The contact angle of a surface against water is of particular interest. One distinguishes between hydrophobic surfaces, where the contact angle Θ is larger than 90° , and hydrophilic surfaces, where the contact angle Θ is smaller than 90° . Here the polarity of the surface plays a major role. Very interesting is the so-called

ultra-hydrophobic behavior, where the contact angle Θ is even larger than 150° and water is strongly repelled. This is achieved by a combination of surface roughness with a hydrophobic surface [3, 8, 34], where the roughness causes an amplification effect for the contact angle. Ultra-hydrophobic surfaces are observed in many cases in nature (wing of butterfly, Lotus leaf, etc.) and often also show self-cleaning properties, i.e., dirt is easily removed by water.

The *interfacial tension* is measured between different polymers or between a polymer and a substrate. In general, it is much more difficult to determine than the surface tension and therefore it only has been measured for specific examples [3]. The reason is that high viscosities of the polymeric materials, long time scales for the achievement of equilibrium, and sample decomposition make measurements for high-molecular-weight polymer materials quite difficult. The determination of interfacial tension, however, allows determination of interface width and compatibility of polymer materials using model assumptions (mean field theory) [1]. In practical cases, typically the pendant or rotating drop techniques are used.

2.3 Functional Polymer Surfaces

The fascinating aspect of functionalization of surfaces is that a very thin nanoscopic surface layer can completely change appearance and functionality of a material while bulk properties are essentially unchanged. This can include wetting, color, hardness, biocompatibility, conductivity, adhesion, friction, corrosion resistance, and many more properties [1–5, 7, 34–37]. It is even possible to generate switching, adaptive, or smart surfaces, which change their properties according to a stimulus. There are various ways to generate functional polymer surfaces. They have in common that a thin layer of a functional material is put at the surface. This can be achieved by chemical bonding, physical adsorption, or segregation of components from the bulk to the surface. It includes the deposition of a coating to the surface which again can be achieved in different ways. This is a wide field and it is hardly possible to cover here all aspects. Several reviews exist [34–37] and we will focus in the following on the particular way of surface functionalization by polymer brushes which form a stable nanoscopic thin layer that is chemically attached to the surface.

With polymer brush layers, one can nicely tune surface properties of materials [34–43]. They can be tightly attached to most materials by the choice of suitable chemistry. With mixed brush layers, it is possible to achieve switching or adaptive properties of the surface. Similarly, one can introduce multifunctionality at the surface by attachment of different chains, nanoparticles, and by incorporation of chemical functional groups.

For this reason, their use has grown over the last years, and polymer brush layers are adopted in several areas of application. This includes for instance flat substrates, but similarly colloidal particles, fibers, or rough surfaces. A big area of application is related to bio-interfaces, where blood interaction, cell growth, or protein adsorption is investigated [36, 41, 43]. This happens in aqueous environment and in many cases water soluble or polyelectrolyte brushes are utilized [38]. Other areas of application

include coatings, where wetting, adhesion, friction, local sensing, or the reflection and emission of light is controlled. Some examples will be discussed below.

We should first define in more detail, what we mean with polymer brushes. The rigorous definition of Alexander and de Gennes [44–46] assumes that brushes are end-attached polymer chains, which are grafted to the surface at high grafting density where the chains are significantly stretched due to mutual interactions. There are much more than one chain in a volume which an unperturbed chain would adopt at the surface (grafting density $\Sigma \gg 1$). It has been shown theoretically and experimentally that chains are highly stretched chains under those conditions and show properties that are significantly different from unperturbed chains [46]. One example is the autophobicity of a so-called dry brush, where free chains cannot penetrate into the brush layer, which even leads to the dewetting of chains of the same kind on top of the brush layer.

We will however not use this rigorous definition, and call already chains with some stretching a brush layer [43, 46]. So we only assume that there are more than one chain in a volume that an unperturbed chain would adopt at the surface ($\Sigma > 1$). The reason is that already this layer can shield the surface nearly completely and that it can be achieved much easier experimentally. There is still sufficient chain mobility left to allow mixed layers to switch and to rearrange their conformation on response to external stimuli. In the following, we will in particular concentrate on mixed brush layers, which can switch and adapt their properties in response to external stimuli.

If we graft two different polymers onto a solid surface, this surface may adopt the properties of one or the other material or in between which can be tuned by external stimuli ([34, 35, 43] and references therein). It even allows to achieve intermediate or new properties. The scheme of switching is schematically illustrated in Fig. 6. Two polymers are attached by covalent bonds to the surface either by

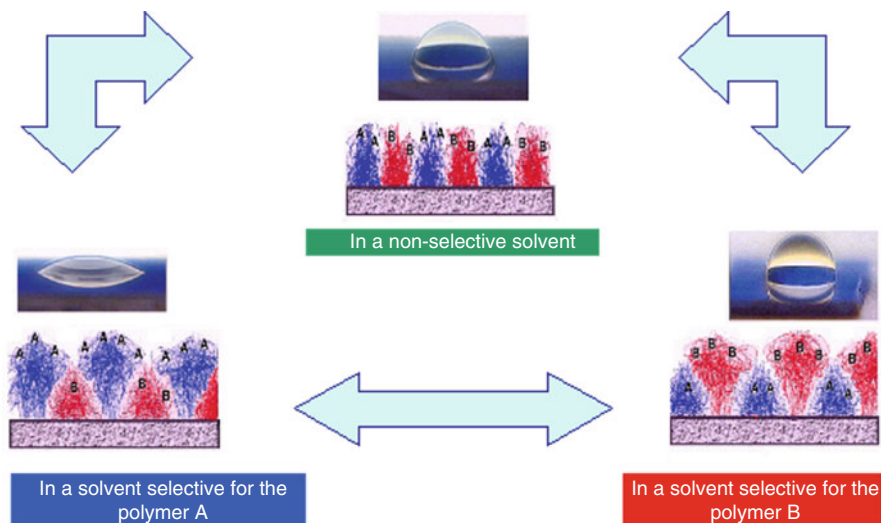


Fig. 6 Scheme of switching of surface properties with polymer brushes with selective solvents [43]. (Reprinted from Ref. [48] with permission from Elsevier)

grafting-to or by grafting-from techniques. One assumes that they are statistically distributed on the surface. The blue polymer could be hydrophilic (e.g., poly(2-vinyl pyridine)) and the red polymer then would be hydrophobic (e.g., polystyrene). In most cases, the two components would be incompatible with each other, but like a copolymer, they only phase segregate at the scale of their molecular dimension. In a solvent selective for the blue polymer (e.g., acidic water), the blue chains are swollen, while the red chains would be collapsed at the surface. There is a complex interplay of lateral and perpendicular phase segregation at molecular level [34], which results in a nanoscopic phase segregation in the surface plane, while the blue polymer might be enriched at the surface. After drying of the film, one might expect hydrophilic behavior, since the wetting is determined by the outermost hydrophilic layer. A water drop on such a surface thus will show a low contact angle.

Exposing this surface to a nonpolar solvent (e.g., toluene), now selective for the red polymer, the situation reverses. The red polymer is typically enriched at the surface, and the dried film might exhibit hydrophobic behavior. The contact angle of water then will be high. This switching is achieved entirely by a conformational change, and therefore is completely reversible. The covalently attached chains cannot perform changes at long range, and they are neither dissolved nor removed, as it could be the case for purely adsorbed molecules. Also intermediate states are possible if one applies less selective solvents.

The situation is however more complex as it might appear at first glance. One definitely needs some chain mobility to achieve switching; chains should be not too short to be able to form a complete upper layer, while they should not be too long to assure reasonable switching times for conformational readjustment. The solvent should partly penetrate the other (upper) component, since otherwise it might not reach the lower layer to cause swelling. Swelling is also difficult, if the grafting density is too high. So there are some limitations and requirements to achieve reasonable switching. Those details of course will largely influence the switching times.

The timescales of switching can vary over a wide range, and have to be adjusted with respect to the application. So switching can be fast (less than seconds), the surface may be called adaptive. A hydrophobic surface then may immediately switch to hydrophilic behavior with exposure to water – and vice versa. For a raincoat, on the other hand, this would not be suitable, and a water repelling brush layer should be stable upon exposure to water and keep the hydrophobic properties. This can be achieved, when the upper brush layer is thick, quite immobile (e.g., in the glassy state), and if this layer is mostly impenetrable to water. The switching times then should be very large (possibly days) and the brush coating is constantly water repelling.

A significant enhancement of the switching effect can be achieved by a combination of surface chemistry and surface topography. The amplification effect causes so-called ultra-hydrophobicity, which is observed at a particular surface roughness. Combining binary brushes with a particular high surface roughness results in a water contact angle that can be switched between virtually 0 and 150 degrees! This is then simply achieved by attaching brushes to a surface with appropriate roughness. In a

model experiment (Fig. 7a), a rough PTFE surface is obtained by etching with plasma. Roughness values can be up to several micrometers. From plasma treatment, one also generates functional groups at the surface, and the mixed polymer brush can be attached by grafting-to technique. After acidic water treatment, the contact angle is close to 0, while exposure to 1,4-dioxane or toluene switches the contact angle to 150 degrees (Fig. 7h). We should note that contact angles of corresponding smooth surfaces switch only between 70 and 90 degrees, and that roughness provides the amplification to smaller and larger contact angles, respectively [43]. In the ultra-hydrophobic state of the brush also the contact angle hysteresis is not observed, which is another criterion for ultra-hydrophobicity.

Using mixed polymer brushes, a wettability gradient can be generated in one or two directions [43, 47]. These brushes are generated by grafting in a temperature gradient which results in a composition gradient. With a linear temperature gradient, the first homopolymers is grafted, and the second polymer is then put into the remaining reactive sites at the substrate. Those gradient brushes can for instance be created with polystyrene PS and the incompatible polyelectrolytes (poly(acrylic acid) PAA, and poly(2-vinyl pyridine) P2VP. The corresponding binary gradient brush shows a gradient of wettability in response to different pH values (Fig. 8). At pH = 2, the wettability gradient proceeds along the P2VP content in the brush. In neutral media, the gradient is essentially “switched off,” whereas it appears again at pH = 9–10 in opposite direction along with increasing PAA fraction. So direction and amplitude of the wettability gradient of a binary polyelectrolyte brush is tuned by pH. These properties may be used for microfluidics or for transport of liquids and particles. Gradient surfaces can similarly be used for separation of binary liquid mixtures. In a lab-on-a-chip [68] device with an integrated FET sensor, the separation of a fluid mixture was achieved.

For many analytical applications, the development of chemical and biological sensors is of interest which includes monitoring of environmental and industrial processes, quality control of nutrition and water, as well as medical and security applications. So the change of fluorescence of organic dyes or the plasmon resonance of inorganic nanoparticles in different environments can be used to detect chemical substances and ions. In this respect, the combination of the responsiveness of polymer brushes and the special properties of nanoparticles turns out to be very interesting for fabrication of thin film sensors (Fig. 9) [43]. As an example, gold nanoparticles may be immobilized via hydrogen bonding on end-functionalized polystyrene brushes (Fig. 9). The presence of the Au nanoparticles on polystyrene brushes was visualized by AFM, XPS, and UV-VIS spectroscopy. By the solvent responsiveness of the polystyrene brushes, the detection of nanoscale optical changes was possible based on localized surface plasmon resonance (LSPR) of the immobilized Au nanoparticles. The change of the proximity of the immobilized Au nanoparticles as a consequence of the solvent-induced reversible swelling-deswelling of polystyrene chains is the basis of the sensing mechanism. The shift in plasmon resonance band caused by variation in the surrounding media is used for sensing, and a chemical nanosensor for the detection of a variety of organic solvents could be demonstrated.

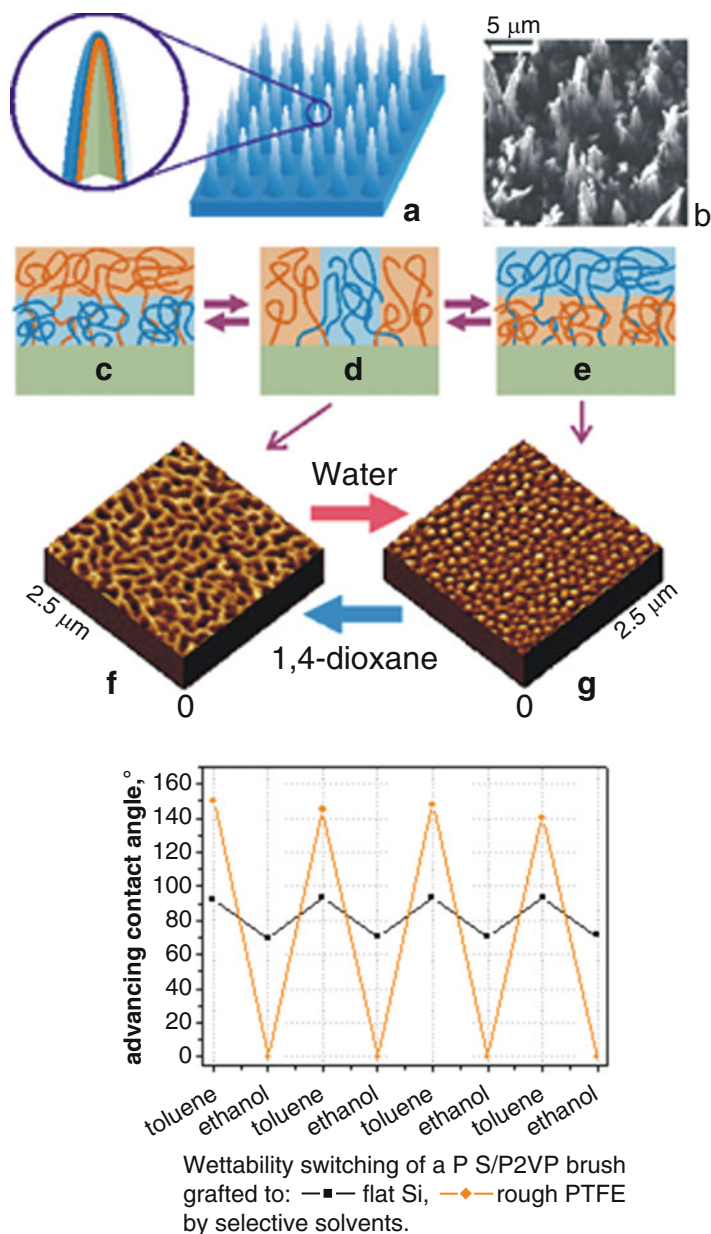


Fig. 7 Two-level structure of a self-adaptive surface: switching of surface properties by a combination of a rough surface morphology and binary brush on a PTFE surface (a–e) where (b) shows the SEM image of the PTFE surface after 600 s of plasma etching. The rough surface is covered by covalently grafted mixed polymer brushes that consist of hydrophobic and hydrophilic chains as shown schematically in (c–e). By the interplay between lateral and vertical phase segregation, the morphology and composition of the surface is switching upon exposure to selective solvents.

Another sensor works with amino-functionalized CdTe quantum dots that are covalently bonded with carboxylic groups of polyacrylic acid brushes via amide bonding. AFM images show a change in surface morphology and roughness before and after the immobilization with NPs. Covalent linkage between the nanoparticles and polymer brushes was investigated with XPS. Photoluminescence spectroscopy and fluorescence microscopy show that the quantum dots retain their optical properties even after the immobilization. The swelling and collapse of the polymer brush layer with nanoparticles attached in different solvents resulted in an intensity modulation of emitted light of the nanoparticles due to interference effects that can be used to detect the swelling of the brush and in this way perform local sensing of solvent quality [49].

Thus, it was demonstrated that the fabrication of straightforward and highly sensitive solvent and pH nano-sensors is possible, based on solvent and pH-induced swelling of polymer brushes coupled with surface plasmon resonance of Au (or Ag) nanoparticles, respectively. The change in plasmon absorption band of immobilized Au/Ag nanoparticles can be detected via UV-VIS absorption spectroscopy where sensitivity is of comparable level as for more complex techniques. Particles have a good adhesion to the polymer support, which minimizes their leakage even after multiple uses and the P2VP-Ag NPs system is quite stable at lower pH. This approach is quite versatile and can be used for the fabrication of nano-sensor devices based on temperature, pH, and ionic strength responsive polymer brushes.

Surfaces with polymer brushes can also be used to control catalytic activity [50]. Catalytically active Pd and Pt NP in P2VP brushes can be synthesized by adsorption of either Pd^{2+} - or PtCl_6^{2-} -ions to the polymer and subsequent reduction to NP by sodium borohydride (NaBH_4). The amount and distribution of nanoparticles on the surface depends strongly on the employed concentrations and length of adsorption and reduction steps. Parameters have to be selected carefully to achieve high surface coverage and ensure the fine dispersion of nanoparticles at the same time. Both Pd and Pt NP show high catalytic activity, which can be switched by use of PNIPAM brushes. The stimuli-responsive catalytic coatings are fabricated by in situ synthesis of metallic nanoparticles in binary PNIPAM–P2VP (poly(N-isopropyl acrylamide)–poly(2-vinyl pyridine)) brushes (Fig. 10). The amount of immobilized nanoparticles is controlled by the polymer ratio, since solely P2VP interacts with the nanoparticles. To investigate the temperature-dependent catalytic activity of the nano-assemblies, the reduction of 4-nitrophenol to 4-aminophenol by NaBH_4 was monitored by UV-VIS spectroscopy as a model reaction. The peak at 400 nm, owing



Fig. 7 (continued) In corresponding solvents, the individual polymers preferentially move to the top of the surface (c and e), while in a common solvent both polymers are present at the surface (d). In f and g, AFM images of the different morphologies after exposure to selective solvents are shown. The amplification effect for contact angle switching for untreated (back) and functionalized (orange) surfaces is shown in (h) [34]. (Reprinted with permission from Ref. [34]. Copyright 2003 American Chemical Society (a–e) and from Ref. [48] with permission from Elsevier (h))

Fig. 8 Scheme of the switching of a wettability gradient obtained from a polyelectrolyte gradient mixed brush (P2VP mixed with PAA) by pH [43]. (Reprinted with permission from Ref. [47]. Copyright 2004 American Chemical Society)

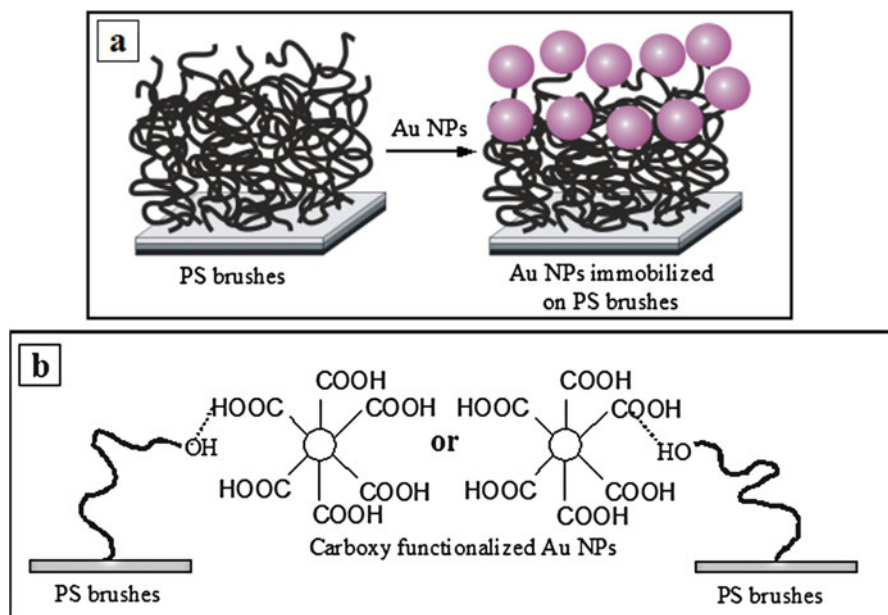
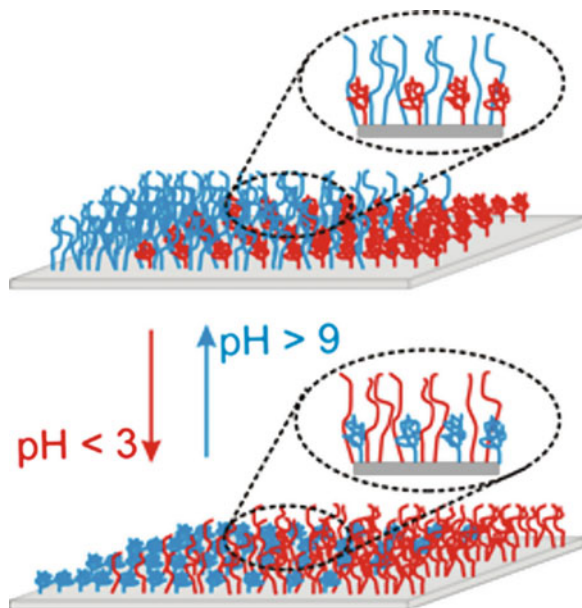


Fig. 9 Sensing by nanoparticles attached to polymer brushes: (a) carboxy-functionalized gold nanoparticles are attached on end-functionalized PS brushes and (b) scheme of hydrogen bonding between carboxy-functionalized Au NPs and hydroxy end groups of PS chain ends [43]

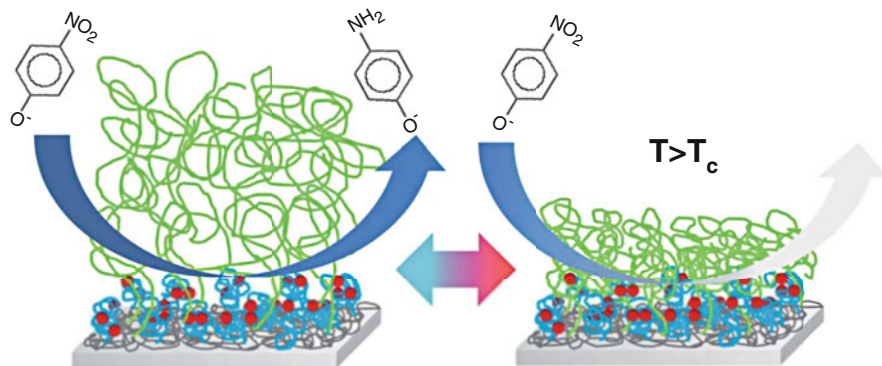


Fig. 10 Scheme of stimuli-responsive catalysis of nanoparticles deposited on binary polymer brushes; the temperature-induced collapse of PNIPAM chains (green) at T_c is proposed to lead to a diffusion barrier blocking the access of reactants to the catalyst (red) [50]

to 4-nitrophenol, decreases and the peak at 300 nm increases with time which indicates the reduction of 4-nitrophenol to 4-aminophenol. Control of the catalytic activity by the temperature-induced deswelling of PNIPAM at T_c is observed, which is explained by the formation of a barrier layer of PNIPAM with increasing temperature. In this way, diffusion of components to catalytic active sites is controlled.

Functional polymer brush layers can be used in various ways to control bio-activity [36, 41]. So adsorption or desorption of proteins as well as cell growth and cell attachment can be performed with polymer brushes. As an example, it was shown that functionalized substrates exhibit cell-guiding properties based on incorporated bioactive signaling cues [41]. The surface was functionalized by polymer brushes made of poly(acrylic acid) PAA, which were functionalized with hepatocyte (HGF) and basic fibroblast growth factor (bFGF) either by physisorption or chemisorption (Fig. 11). The GF release kinetics shows a high initial burst followed by a constant slow release in the case of both physisorbed HGF and bFGF. In contrast, chemisorbed HGF remained bound to the brush surface for over 1 week, whereas 50% of chemisorbed bFGF was released slowly. These GF-functionalized PAA brushes produce a measurable effect on human hepatoma cell lines (HepG2) and mouse embryonic stem cells (mESCs) and can be used as bioactive cell culture substrates to tune cell growth and differentiation.

3 Interfaces in Blends, Copolymers, and Composites

The interfaces between polymers in blends and copolymers as well as between polymers and mostly solid components of composites (typically particles and fibers) determine to a large extent the properties of the materials [1–5]. The interfacial region, which is formed between phases of an immiscible polymer blend, will influence the mechanical behavior of the blend under stress. Similarly the adhesion

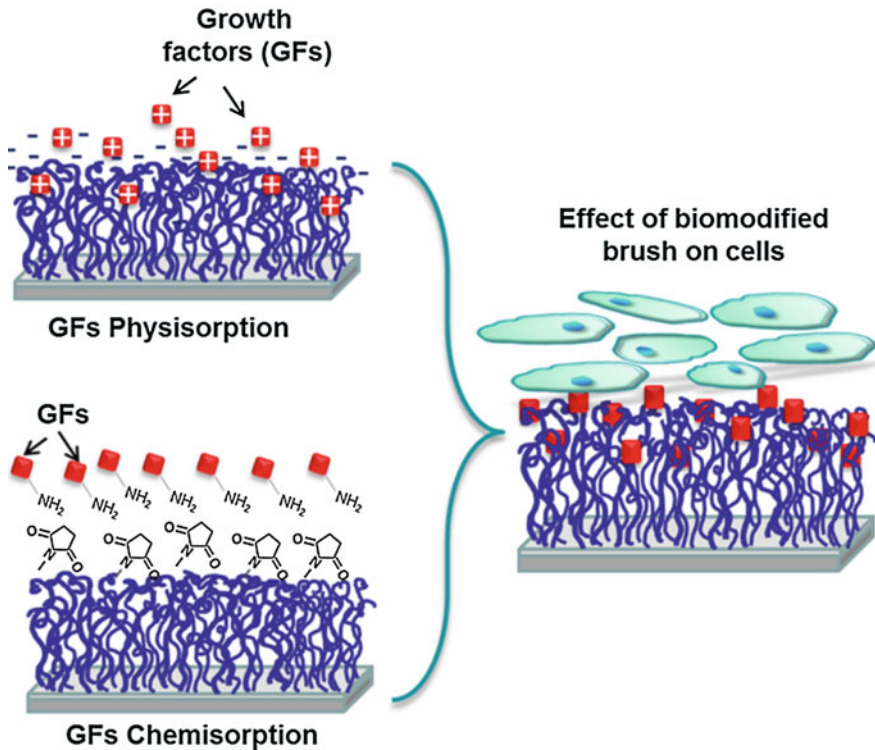


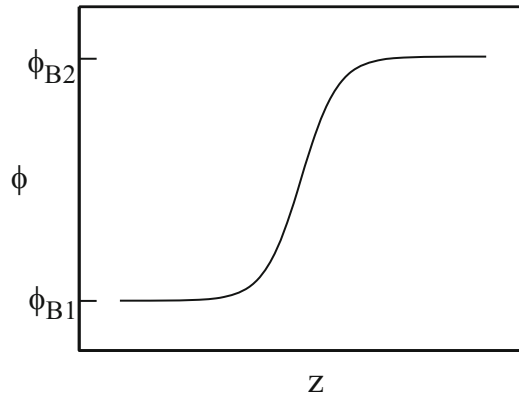
Fig. 11 Grafting of pol(acrylic acid) PAA as brush on solid substrates: Bio-functionalization of PAA brush with growth factor (red squares) through physisorption or chemisorption (left). Interaction of GF-modified PAA brush with HepG2 cells (for HGF-PAA) or mESC's cells (for bFGF-PAA) (right) [41]

between particles or fibers and the polymer matrix of a composite will influence the strength of the composite. So we first shortly discuss the theoretical background and then provide some examples. The investigation of interfaces inside of bulk materials turns out to be much more complicated than the investigation of surfaces. We discuss some experimental techniques in Sect. 4.

3.1 Interfaces Between Homopolymers

When two polymer sheets are put together in the melt, an interface is forming. The width of this interface depends on the chain compatibility and determines for instance the adhesion between the sheets [1–5, 8–10, 12, 13]. If the two polymers are compatible, they will interdiffuse with each other and depending on diffusion time and diffusion coefficient at given temperature, an interface will form. This is typically controlled by Ficks law. The situation is however more complicated at short interdiffusion times and if the two polymers are chemically different or possess

Fig. 12 Interface profile between the phases of a blend of two incompatible polymers. The concentrations of the polymers in the blend are Φ_{B1} and Φ_{B2} , respectively, and are determined by the phase diagram. Z is a spatial coordinate across the interface [51]



different mobility (e.g., different molecular weight). Taking chain reptation into account with different diffusion laws at different time scales and the enhancement of chain ends at the surface, a different interdiffusion behavior is expected at small diffusion times. Similarly the situation becomes more complicated, if mobilities of the two polymers are different. The mean position of the interface will move and an asymmetric profile will form. For the development of adhesion, the formation of entanglements during interdiffusion is important. There are plenty of investigations of those effects. At longer diffusion times, the compatible polymers will intermix and at thermodynamic equilibrium form a homogeneous blend.

Most polymers are however incompatible with each other and blends of polymers will be inhomogeneous in nature [10, 12, 13, 51]. Phase segregation between components will occur and only small interfaces between the phases will form. These interfaces between incompatible polymers are typically in the range of 2–50 nm, depending on compatibility. We first will provide a short introduction to mean field theory of interface formation and interfacial tension, and then present some specific examples. Experimental methods employed for the investigation of polymer interfaces are important to gain an understanding and will be discussed in the following Sect. 4 with respect to their accuracy and advantages, with emphasis on neutron- and X-ray reflection, electron microscopy, ellipsometry, interfacial tension, and nuclear reaction analysis techniques.

For most incompatible materials, the interface is not very wide depending on compatibility [3, 10, 12, 13, 51]. A typical interface profile is shown in Fig. 12. When two incompatible polymers are put into contact, segments will move if the materials are heated above the glass transition, and some interpenetration will occur. Therefore the interface width increases with time and reaches an equilibrium value, which is determined by the Flory-Huggins interaction parameters χ according to mean-field theory. The quantity χ expresses polymer compatibility, while it is not completely understood on a molecular basis. In practice, it is often used as an empirical parameter and then allows a thermodynamic description of phase separation for a particular polymer pair within mean-field theory. Besides equilibrium thermodynamic effects, other factors originating from sample preparation and

experimental conditions also influence interface formation. When two films are put together to form an interface, there is the influence of initial surface roughness, surface composition, contaminations, and chain conformation at the surface of the films, which may largely depend on sample history. In specific cases, it is difficult to reach equilibrium, for instance, when segment mobility is slowed down by the glass transition T_g .

When comparing experimentally determined interface widths with calculated ones, e.g., from interfacial tension data, one must be cautious, because there are influences from end-group effects, molecular weight distributions, chain orientation, capillary waves, or initial interface roughness that are not very well understood. We also assume that additives like antioxidants or plasticizers are not present, since those materials might migrate to the surface or interface even if present only in trace amounts.

The description of phase behavior in polymer blends is of fundamental interest in polymer research [10]. A first approach is based on Flory, Huggins, and Staverman (FHS) theory. Using a lattice model, a simple form for the free energy of binary polymer blends including the interaction parameter is derived

$$\frac{F_{FHS}}{kT} = \frac{\phi \ln \phi}{N_1} + \frac{(1 - \phi) \ln(1 - \phi)}{N_2} + \chi \phi (1 - \phi) \quad (3)$$

N_1 and N_2 are the degrees of polymerization and ϕ the volume fraction of one of the polymers. The interaction parameter χ is related to the interactions between segments. It is on the other hand an effective interaction parameter, which takes into account the difference between interactions of the same and different segments of the blend. So it typically is very small quantity although the actual interaction energies are much larger. Many theories have been derived to describe the interaction parameter as a function of temperature to reproduce phase diagrams observed in different experiments. For complicated phase diagrams, it may be necessary to introduce a ϕ -dependence of χ in addition. Equation 3 now contains first the entropic terms, which are small at large N , and second the enthalpic term with χ , which includes the interaction energies and which dominates the free energy. As a consequence, most polymers are immiscible with each other.

In order to discuss the problem of an interface between two polymers [10], Equation 3 has to be extended by the so-called quadratic gradient term $\kappa(\nabla\phi)^2$ introduced by Cahn and Hilliard to take fluctuations into account. This allows the derivation of the equilibrium volume fraction profile. An analytical solution for the volume fraction profile can be calculated for the case of infinite degrees of polymerization ($\chi N \gg 1$), which is equivalent to strong segregation,

$$\phi(z) = \frac{1}{2} \left(1 + \tanh \frac{z}{l} \right) \quad (4)$$

with

$$l = \frac{a}{\sqrt{6\chi}} \quad (5)$$

a is the mean characteristic segment length of the polymers. So even for strong segregation, the two components interpenetrate over some distance. In the same approximation also the interfacial tension γ depends on χ

$$\gamma = \frac{kT}{a^2} \left(\frac{\chi}{6}\right)^2 \quad (6)$$

A simple way to estimate the influence of finite chain length is possible for the case of two polymers with the same degree of polymerization N

$$l = \frac{a}{\sqrt{6\left(\chi - \frac{2}{N}\right)}} \quad (7)$$

As a result, the interface width l and the interfacial tension γ are directly related to the Flory Huggins Stavermann effective interaction parameter χ . For the experimental determination of l , one has to be careful, however, since besides this intrinsic interface width also lateral fluctuations are depending on interfacial tension and consequently on χ . In many cases, it is difficult to distinguish between “intrinsic interface” and capillary wave effects. This is reflected in computer simulations where both effects contribute to the apparent interface width and a correction of the measured interface width with respect to capillary waves is necessary.

As mentioned before, the interface width may be determined by neutron reflectometry [51, 52], if one of the components has been deuterated and a contrast at the interface has been generated. Two highly smooth films are put on top of each other and after annealing in the melt the interface width is determined.

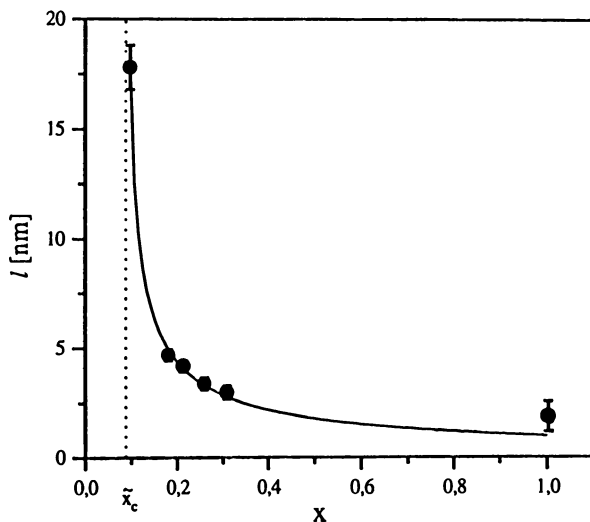
One of the most intensively studied incompatible blend systems is poly(styrene) PS versus poly (methyl methacrylate) PMMA. Values of interface widths l determined with different techniques are of the order of $l = 1.3$ nm [51]. The most accurate value has been obtained with neutron reflectometry from a blend system and has been confirmed from studies of diblock copolymers, where the interface width between lamellae is found to be of the same size. Also, temperature-dependent ellipsometry investigations and TEM yield similar results within error bars. A serious discrepancy, however, arises when the interface width is calculated from interfacial tension data on the basis of meanfield theory. Those interface widths are approximately a factor of two smaller than the measured ones. This might indicate that capillary wave effects might significantly contribute to experimental values, which may contain “intrinsic” and capillary wave effects as discussed above. Of course also other effects could contribute like end-group effects, conformational changes or surface contaminations.

Several other systems have been investigated including interfaces between compatible polymers [51, 52]. Theory predicts at initial stages of interdiffusion a special behavior due to reptation effects. In reptation theory one assumes that initially chains diffuse across the interface mostly via chain ends, which results in a particular time dependence of the growth of the interface width. Other studies deal with partially compatible polymers or blends, where one of the components is in the glassy state.

The blend system of PS and the statistical copolymer poly(styrene-statpara bromo styrene) $\text{PBr}_x\text{S}_{1-x}$ [51] was chosen for systematic investigations of the dependence of interface width on compatibility. Here compatibility between components can be adjusted between completely compatible to highly incompatible by a change in degree of bromination x . Since materials can be obtained by bromination of polystyrene with narrow molecular weight distribution, where the degree of bromination can be high, the contrast between components may be sufficient also for X-ray reflectivity experiments. However, at low degree of bromination, deuterated PS has to be utilized, and NR experiments are performed. The results from all experiments are shown in Fig. 13. At low x , the interface width diverges because the system becomes compatible at x_c . The functional form is fitted empirically by a composition-dependent χ -parameter, which contains the concentration-weighted individual segment-segment interaction parameters of the components. Values at large χ can be compared to other X-ray and neutron reflectivity data. There is good agreement between different data sets and theory, where mean field theory is used to calculate the interface width at different compatibility. Also, the influence of the glass transitions on the interface width has been studied, since the glass transition also increases with degree of bromination. If the sample is annealed between the glass transitions of the components, segment interdiffusion is strongly reduced. In this temperature regime, the interface width depends strongly on temperature until both components become mobile and the glass transition temperature also of the second component is reached. At higher temperatures, dewetting phenomena are observed that are a consequence of the strong incompatibility of the components.

Copolymers are also used for compatibilization of incompatible polymer blends, where a small addition of a diblock copolymer can significantly improve the mechanical properties of the blend [3, 53, 54]. This is due to the fact that the diblock copolymer might be enriched at the interface and provides a mechanical bridge

Fig. 13 Dependence of interface width l on degree of bromination x for the blend system PS versus $\text{PBr}_x\text{S}_{1-x}$. The system becomes strongly incompatible at large x , while it is compatible for $x < x_c$ [51]



between the segregated phases of the two components where interface width and mutual interpenetration otherwise are small. It has been predicted by theory [53] that the diblock copolymer will be enriched at the interface and that the interface is broadened by addition of the copolymer. It is assumed that the two blocks are compatible with the corresponding homopolymers of the blend. With neutron reflectometry or nuclear reaction analysis, those predictions can be tested [54] by utilizing dedicated contrast generation by deuteration: (i) the enrichment of the copolymer at the interface can be visualized if the copolymer has been deuterated with otherwise nondeuterated homopolymers, and (ii) the broadening of the interface is resolved if one of the homopolymers and the corresponding block of the copolymer have been deuterated with otherwise nondeuterated components.

Thin films of copolymers are used in various ways for generation of nanostructures at surfaces [55–57]. The two incompatible blocks phase segregate at the scale of the molecules and form nanoscopic ordered morphologies. The interface to the substrate is important for adhesion but also for alignment of the nanostructured films, while the surface to air determines the wetting behavior and other properties. A particular example are structures formed by a supramolecular approach (SMA) with diblock copolymer thin films of polystyrene, poly(4-vinyl pyridine) PS-*b*-P4VP and 2-(4'-hydroxybenzeneazo) benzoic acid HABA, which is a low molar mass additive associated with one of the blocks by noncovalent interactions [56–58]. This low molar mass additive is removed easily by selective dissolution from the P4VP phase to obtain a nanoporous ordered thin film. SMA with block copolymer self-assembly is a simple and powerful technique for fine tuning of block copolymer morphologies, and has been successfully used in bulk and in thin films. Figure 14 shows the schematic representation of the formation of nanotemplates by this technique. A solution of PS-*b*-P4VP block copolymer and HABA was spin cast on to a silicon wafer as a thin film. A cylindrical morphology was observed either with the cylinder axis parallel or perpendicular to the substrate where orientation

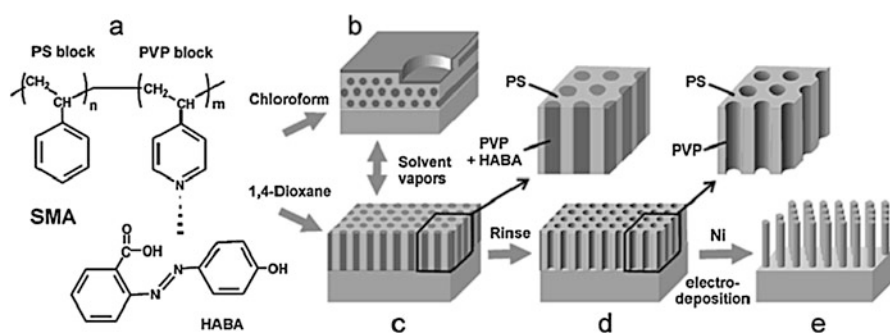


Fig. 14 Generation of ordered nanotemplates with diblock copolymer thin films: the supramolecular assembly SMA of PS-*b*-P4VP block copolymer and HABA (a) is formed by solvent casting. Depending on the solvent, perpendicular (c) or parallel (b) alignment of the structure is achieved. The nanotemplate (d) is prepared by dissolution of HABA. The empty cylinders can be filled by electrodeposition with nickel, and the polymer matrix removed by dissolution in toluene (e) [56]. (Reprinted with permission from Ref. [59]. Copyright 2003 American Chemical Society)

depends on the solvent. By exposure to different solvent vapors, the orientation of the cylindrical microdomains of P4VP(HABA) could also be switched. Annealing in chloroform results in parallel, and annealing in 1,4-dioxane results in perpendicularly oriented cylinders. HABA can be removed from the SMA thin films by immersing in ethanol to transform the block copolymer thin film into a nanotemplate [59]. Due to specific interactions, the P4VP material is enriched both at the surface and at the interface to the silicon wafer. The nanotemplate may be further processed and for instance filled with nickel by electrodeposition. After removal of the polymer matrix the ordered nickel nanorods are left over.

The combination of block copolymers with nanoparticles can add additional functionalities to those coatings. The first commonly used way to prepare hybrid polymer/inorganic nanocomposites is to directly mix presynthesized and suitably functionalized nanoparticles with block copolymers and then allow the whole system to self-assemble [7, 56–61]. Nowadays, nanoparticles of various chemical compositions can be synthesized in solution with precise control over size and shape. The nanoparticles should be stabilized against aggregation and coalescence either electrostatically or sterically by coating with ligands that bind to or adsorb onto the NP surfaces. These ligands might be small molecules, functional (co)polymers, polyelectrolytes, or biomolecules that control interfacial interaction. Such core-shell particles are combined with block copolymers, e.g., by dissolving in common solvent and allowing solvent to evaporate. In particular cases, annealing steps might be required to bring the whole system to an equilibrium state. To achieve domain-selective localization, the particle/polymer interactions are tuned such that particles prefer one block copolymer domain over another. Hydrophobic, electrostatic, or hydrogen bond interactions between monomer units or functional groups can promote domain-selective nanoparticle localization. Various types of inorganic nanoparticles stabilized with small organic molecules can be incorporated in different domains of block copolymers matrices using direct mixing approach. As an example, iron oxide nanoparticles stabilized with oleic acid were selectively segregated into PMMA domains of self-assembled PS-*b*-PMMA matrix [57], but many other examples are reported.

So one can fabricate highly ordered arrays of nanoscopic palladium dots and wires (Fig. 15a) by the direct deposition of presynthesized palladium nanoparticles in aqueous solution [56]. As mentioned before, the cylindrical morphology observed in thin films of PS-*b*-P4VP can be switched from parallel to perpendicular and vice-versa by annealing in vapor of appropriate solvents. By immersion into ethanol, a good solvent for P4VP and a nonsolvent for PS, surface reconstruction of the films was observed with a fine structure. Perpendicular cylinder alignment resulted in a nanomembrane with hexagonal lattice of hollow standing cylinders, and parallel cylinder alignment produced nano-channels. Figure 15b shows AFM height images of nanopores and nano-channels after surface reconstruction. In these templates, the pore or channel walls are formed by functional P4VP chains. A subsequent stabilization of the polymer matrix by UV-irradiation followed by pyrolysis removes the polymer matrix material and produces highly ordered metallic nanostructures. Figure 15c shows AFM height images of palladium nano-dots and nanowires after the removal of the polymer matrix. This method provides a facile approach to fabricate a broad range of

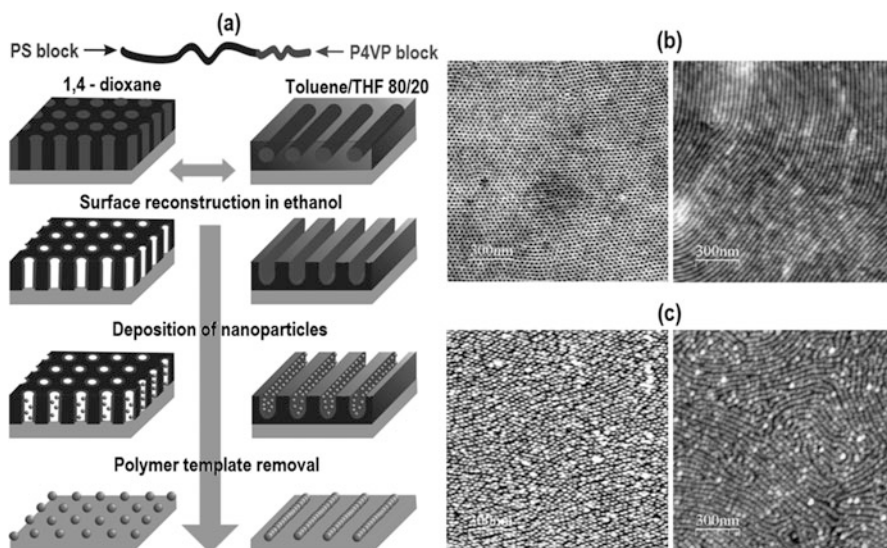


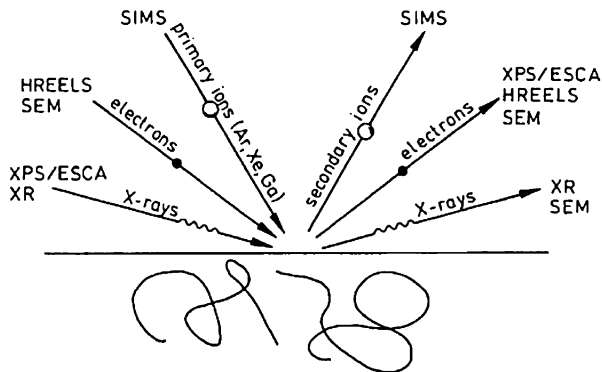
Fig. 15 (a) Schematic diagram of the fabrication process of ordered arrays of nanoscopic palladium dots and assemblies using block copolymer template. (b) AFM height images of PS-b-P4VP nano-templates with perpendicular and parallel arrangement of nanostructures obtained after surface reconstruction in ethanol. (c) AFM height images of palladium nanodots and linear assemblies obtained after the polymer matrix removal [56]. (Reprinted from Ref. [60] with permission of Elsevier)

nano-scaled architectures with tuneable lateral spacing, and can be extended to systems with even smaller dimensions. One can also pattern noble metal nanoparticles such as gold, platinum, and palladium. It is also possible to deposit differently functionalized nanoparticles in or respective on top of the different phases of block copolymer thin films [58]. Also ordered arrays of nanoparticles can be produced inside of the confined space of block copolymer cylindrical phases [60, 61] and nano-objects formed by selective solution [7]. Glass and carbon fibers are widely used for mechanical reinforcement to achieve lightweight materials with good mechanical properties, and oxydic, metallic, or semiconducting nanoparticles are applied for optical, electrical, magnetic, catalytic, or sensing applications. Dispersion and contact of fibers or nano-particles with the surrounding polymer matrix are again highly important, which are determined by the interface between them. The analysis of those interfaces is particularly difficult because properties of the organic and inorganic components are very different.

4 Characterization Techniques of Polymer Surfaces and Interfaces

The characterization of polymer surfaces and interfaces is a difficult task and needs dedicated techniques [1, 3, 11, 20, 32, 51, 52, 62–67]. This is in particular true for the characterization of interfaces, which are hidden inside of the material. To get a

Fig. 16 Schematics of some surface characterization techniques where different types of radiation are used for incident and outgoing beam [3]



reasonable picture, usually a combination of different techniques is necessary. Some of the most common techniques are schematically depicted in Figs. 16 and 17 and listed in Tables 1 and 2, where also typical resolution and information obtained is provided. Those data are however only rough guides and resolution for instance can be much worse or better depending on sample preparation and particular instrumentation used. As an example, for a polymer blend surface, the wetting properties are determined by contact angle measurements, which may provide already a hint on surface composition or segregation of components, the roughness, and lateral nanostructure is determined by scanning force microscopy, the detailed surface composition by x-ray photoelectron spectroscopy, the morphology in the vicinity of the surface by x-ray reflectometry or in more detail by grazing incidence x-ray scattering, and mechanical properties of the surface by nano-indentation. One might of course not need all this information, and characterization techniques have to be carefully chosen for a particular question. Several other and more dedicated techniques are available, which may provide better resolution or additional information, but mostly require more dedicated instrumentation and in many cases also special sample preparation.

From the time dependence of interface formation, one can learn about segment mobility and interdiffusion mechanisms. Techniques are needed that can resolve details of the interface between polymeric components at nanoscopic level. Since the interface width for incompatible polymers is typically much smaller than 50 nm, the resolution of the technique has to be adapted for a determination of such small interface widths. To achieve good resolution, a suitable contrast between components has to be present in order to “see” the interface between the components. Such a contrast can be generated for neutron reflectometry (NR), for example, by deuteration of one of the components [1, 3, 52]. So in multicomponent systems, one particular component and its interfaces with other components can be made visible for neutrons. The application range may be limited by the particular sample geometry needed. Other techniques include ellipsometry, small angle scattering, ion techniques, electron microscopy, and measurements of interface tension.

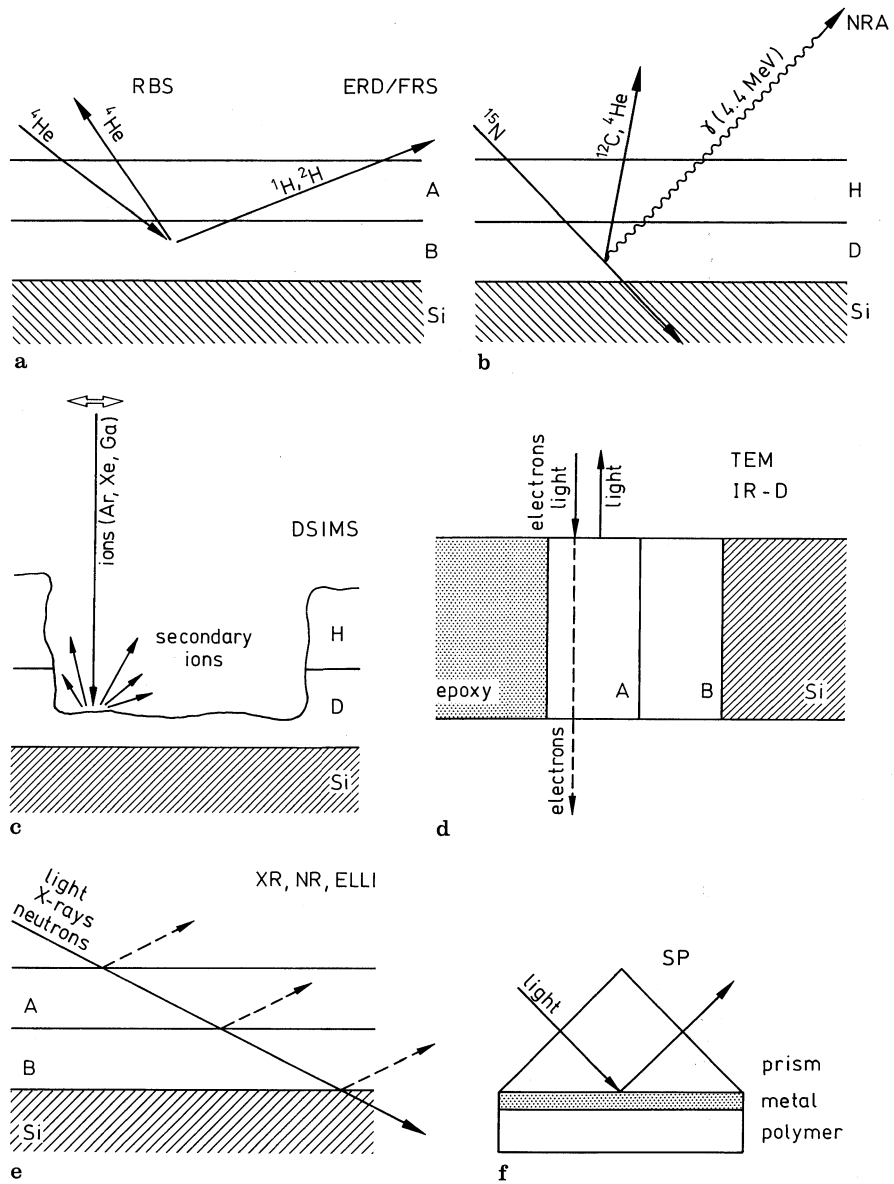


Fig. 17 Schematics of several surface and interface analysis techniques: (a) Rutherford backscattering (RBS), (b) nuclear reaction analysis (NRA), (c) dynamic secondary ion mass spectrometry (DSIMS), (d) transmission electron microscopy (TEM), (e) x-ray (XR) and neutron reflectometry (NR) as well as ellipsometry (ELLI), and (f) surface plasmon spectroscopy (SP) [3]

4.1 Surface and Interfacial Tension

The measurement of surface tension is still one of the easiest and most common techniques for a first surface characterization [3, 8, 32]. Experimental techniques and problems have been discussed in Sect. 2.2. For a detailed surface analysis, other techniques should be used in addition.

The measurement of interfacial tension of polymers is much less straightforward and is determined mostly only in special cases of low-molecular-weight materials.

4.2 Scanning Force Microscopy (SFM)

Scanning force microscopy has been developed as a very versatile technique with many modes for a variety of applications [3, 62, 63]. It provides nanoscopic resolution both in width and height at the surface of a film or substrate, and for instance single polymer molecules adsorbed on a smooth solid substrate have been resolved. Available operation modes include contact, noncontact, hard/soft tapping, materials, adhesion, phase, friction or chemical contrast, indentation, soft or force-distance mode, use of tunneling current, electrostatic, electro-chemical or magnetic interactions, it can be operated in different environments including vacuum, air, liquid or inert/humid atmosphere, and offers various fascinating and versatile possibilities. Nanoscopic resolution of different aspects of a surface can be obtained. So one can measure and visualize the surface with respect to topography, surface hardness, friction, adhesion, conductivity, electrostatic charge, or magnetism. By different operation modes ranging from noncontact to hard tapping, the strength of the interaction of the tip with the substrate can be controlled. To perform depth profiling, the surface can be removed by etching or dissolution techniques, and in this way structures inside the sample and at hidden interfaces may be resolved.

With the tip, individual molecules and atoms at the surface can be manipulated, and for example single atoms may be positioned on a solid surface by the tip. It therefore may not only be used as an analytical but also as a nano-manipulation tool. Its strength comes from the fact that a lateral image can be obtained relatively easily at nanoscopic resolution by different modes, while surface properties at quantitative level are not easy to obtain with this technique. It can be combined with other techniques. Tip-enhanced Raman spectroscopy provides local chemical information, where by plasmon effects at the AFM-tip a local signal enhancement up to a factor of 10^{10} may be achieved, which allows measurement of Raman signals from nanoscopic small spots. An analogous technique is nano-IR, where the local thermal expansion by an IR-beam is detected at nanoscopic level.

A similar technique is scanning tunneling microscopy where the tunneling current between tip and surface is measured and used for tip control. It requires however conductive samples like metals or semiconductors, while nonconducting polymers have to be covered with a conductive layer for measurement. Spectroscopic information is obtained with scanning near-field optical microscopy, SNOM, where a

particular optical fiber is used as a light guiding tip to illuminate the sample. The emitted or absorbed light is then analyzed.

4.3 Ellipsometry (ELLI) and Surface Plasmon Spectroscopy (SP)

Ellipsometry can be used to measure the thickness and index of refraction of a thin layer on a substrate with high precision (the thickness resolution can be better than 1 nm depending on optical contrast) and as a function of time. The change of the polarization state of reflected light from the surface is determined, which provides information on the optical properties of the reflecting medium (Fig. 17) [3, 62]. For very thin films, however, the thickness and index of refraction cannot be measured independently and the so-called optical thickness is determined. For thicker films the technique then reveals thickness and index of refraction of the layer independent from each other (thickness typically larger than 10–20 nm), and may provide information on anisotropy and roughness. By direct ellipsometric imaging (microscopy) or scanning techniques, lateral information on thickness or index of refraction variations at micrometer scale can be resolved too. Problems and limitations may occur from correlations of thickness and index of refraction, low optical contrast in multilayer samples, but also from ambiguities in the evaluation of data in more complex situations, where due to limited experimental data detailed information on the system is difficult to extract. Then spectroscopic or variable angle ellipsometry provides additional information and may help in determination of system parameters. Measurements can be performed under various environmental conditions including for instance the adsorption kinetics of molecules in solution at a solid substrate which may be measured in-situ with a liquid cell. IR ellipsometry can be performed by use of IR radiation from a synchrotron source, which can even provide chemical information in monolayer polymer films or elemental composition.

Surface plasmon spectroscopy (SP) is a very similar technique (Fig. 17) while it uses surface plasmons in a thin metal layer, which are excited by the incident light. The plasmon resonance is influenced by the adjacent polymer layer, which in this way can be analyzed with respect to polymer film thickness and index of refraction. Information content of SP is comparable to ellipsometry, but requires a metallic layer for the excitation of the plasmons.

4.4 Scanning and Transmission Electron Microscopy (SEM, TEM)

Scanning electron microscopy (SEM) [3, 62, 64] is used in scanning and reflection mode for surface investigations. SEM reveals an image of the surface typically at nanometer lateral resolution, and contrast is obtained by electron scattering, absorption, or emission. An image of the element distribution is achieved for instance by electron energy loss (EELS) or x-ray fluorescence spectroscopy (EDX). With organic materials, the sample degradation by the electron beam has to be considered (but also can be used for contrast generation and electron lithography). Contrast and

resolution may be improved, when the surface is covered by a thin conducting film, sputtered at an angle with respect to the surface normal to obtain shading effects. In most cases, quantitative analysis of SEM images is however difficult.

Transmission electron microscopy (TEM), may be used to investigate bulk materials and interfaces where typically a 50 nm thick slice (Fig. 17) is prepared. This slice can be cut with a microtome (using a diamond knife, possibly under cryo-conditions) or with an ion beam (FIB, see below). After staining or other contrasting methods, the interface between materials may be resolved. Limits of resolution arise from intrinsic TEM resolution, but also from preparation, where artefacts and smearing of the interface may occur. Chemical and elemental resolution is obtained using inelastic electron scattering (electron energy loss spectroscopy, EELS) or x-ray emission (EDX). The sample has to withstand ultra-high vacuum during measurement and electron beam damage. For liquid or sensitive samples, cryo-techniques are adapted where the sample slice is shock-frozen and cooled during the experiment. With special setups, experiments at atmospheric conditions or in liquid state are feasible, but require dedicated sample environment with thin windows. TEM however needs in all cases a very special sample preparation, which may be time consuming and difficult to achieve.

4.5 X-Ray Photoelectron Spectroscopy (XPS)

X-ray photoelectron spectroscopy (XPS) can be used to characterize the chemical composition of polymer surfaces. Due to limited electron emission depth, with polymers typically a depth of up to 7 nm is probed [3, 62, 65]. In some cases the acronym *ESCA* for *electron spectroscopy for chemical analysis* is used indicating the possibility of chemical analysis as well as the combination of photoelectron and Auger electron peaks in observed spectra (electron spectroscopy). Electrons from the inner shells or valence bands of the sample are excited and ejected by the incident soft X-rays. The number of photoelectrons which are leaving the sample surface is measured as a function of incident energy. The emission depth of the electrons from the sample is limited, which determines the depth resolution. The measured energy spectrum of the electrons then is characteristic for elemental composition and binding state of atoms of the sample. One can quantitatively determine the surface composition and binding of different species. Measurements are performed under vacuum, and with nonconducting surfaces surface charging has to be avoided.

With conventional scanning XPS instruments, the lateral resolution is typically not better than several micrometers. It may be significantly improved using X-ray photo electron emission microscopy (XPEEM), where an electron microscope is used to image the outgoing electrons. Here the lateral resolution may be of the order of 10–30 nm, when soft x-rays from a synchrotron source are used. Similarly a synchrotron source is needed for transmission x-ray microscopy (TXM), which utilizes the absorption of soft x-rays in a thin film sample for lateral imaging of chemical composition at similarly good resolution.

4.6 Electrokinetic Methods (Zeta Potential)

The preferential adsorption of cations or anions, the dissociation of surface groups, the adsorption of polyelectrolytes, the isomorphic substitution of cations and anions, and the accumulation or depletion of electrons determines the electrokinetic potential on the surface of a solid in contact with a polar medium (usually water) [3]. Usually, one assumes the presence of an electric double layer consisting of two regions of charge distribution at an interface: first a fixed layer and second a diffuse layer. A “surface of shear” or “slipping plane” is located between these two layers. An externally applied electric or mechanic force causes a relative movement between the fixed layer and the diffuse layer. The electrokinetic or zeta (ζ) potential is the potential at this surface. The electrokinetic potential can be measured by applying an external electric field, which results in relative movement of the solid and liquid phases (electrophoresis, electro-osmosis), which generates an electric potential or produces an electric current (called streaming potential/streaming current, sedimentation potential). This can be measured with several experimental techniques, but with planar surfaces often the streaming potential is determined.

4.7 Infrared Spectroscopy (ATR-FTIR)

Infrared spectroscopy provides chemical information and is used for surface and thin film investigations in reflection or attenuated total reflection mode (ATR-FTIR) [3]. Quantitative determination of composition or binding states via vibrational modes is possible. So it is a powerful analytical tool for detection of dynamics at solid/liquid or solid/air interfaces. ATR-FTIR utilizes multiple reflections from a large smooth crystal. The reflecting plane between crystal and surrounding medium is investigated. The IR beam is totally reflected at this interface, but still an evanescent wave penetrates the surrounding medium. Molecules can be distinguished by their IR-spectrum, and deuteration is sometimes used to differentiate between different constituents. The evanescent wave typically penetrates of the order of the wavelength into the other medium, and therefore probes a depth of several micrometers. Utilizing an IR-microscope the lateral resolution similarly can be several micrometers. With an IR array detector, spectroscopic information can be obtained at high speed and spatial resolution. IR synchrotron radiation again enhances time resolution, and allows use of IR ellipsometric imaging techniques for measurement of composition, thickness, orientation, and index of refraction of surfaces and thin films [66].

4.8 Raman Spectroscopy

With Raman spectroscopy also the chemical composition at the surface may be detected [3]. In contrast to IR spectroscopy, those vibrational and rotational states are detected where the polarisation is changing. Since the energy shift of the

scattered light is detected, the observed signal is not so strong and powerful lasers are needed for the investigation of surfaces. With surface enhanced Raman spectroscopy (SERS) the surface signal however can be enhanced by many orders of magnitude. The plasmonic enhancement from metallic nanoparticles (preferentially Ag) is used which are deposited on the surface, and Raman spectroscopy becomes sensitive to the direct environment of those particles [69].

4.9 X-Ray and Neutron Reflectometry (XR, NR, GISAXS)

X-ray and neutron reflectometry techniques (XR, NR) use the fact that x-rays and neutrons are reflected at interfaces (Fig. 17) when a suitable contrast is present [1, 3, 52]. The difference in electron density between materials provides a contrast for x-rays, and x-rays are in particular sensitive for the surface of thin films against air or vacuum. The electron densities between polymers are in most practical cases not very different, and XR cannot easily resolve the interface between two polymer films. The contrast for neutrons on the other hand can be generated by deuteration of one component, i.e., all hydrogens are replaced by deuterium, which chemically is essentially identical to hydrogen, and the interfaces between polymers can then be resolved at nanometer resolution. Both techniques however cannot easily distinguish between lateral fluctuations of the interface (generated by thermal fluctuations, surface roughness, or capillary waves) and the “true” interface (generated by interdiffusion between components). Since both quantities can be in the nanometer range, a quantitative interpretation of reflectometry data in terms of interface width may be difficult (see Sect. 3.1). A separation between interdiffusion and lateral fluctuations may not be necessary however in many cases. Both techniques can on the other hand provide valuable information on film thickness, surface and interface roughness, capillary waves, surface segregation and profile of components in a blend, interdiffusion, interface width and asymmetry etc. The sample should be smooth and flat, and extend laterally typically over several cm. XR and NR can provide information even at sub-nanometer resolution if the quality of the sample (smoothness) is perfect.

For Grazing Incidence Small Angle X-Ray Scattering (GISAXS), two techniques are combined: Grazing Incidence Diffraction (GID), which uses reflection geometry to obtain diffraction from the surface and near surface region, and Small Angle X-ray Scattering (SAXS), which obtains electron density fluctuations and structures at 1–100 nm length scales typically in normal transmission mode. Experiments are carried out close to the critical angle for total external reflection, which results in a considerably enhanced surface sensitivity. The full potential of GISAXS is obtained when it is performed with synchrotron radiation and an area detector. GISAXS is a nondestructive structural probe like other reflectivity and scattering techniques and does not require a conducting surface or special sample preparation. With flat samples GISAXS yields excellent sampling statistics and averages over macroscopic regions while it provides information on lateral nanostructures close to the surface, size distributions, particle geometry, and spatial correlations. Similarly neutrons

can be used at grazing angles (GISANS), but this technique requires high flux neutron sources.

A careful analysis of the decay of the small angle x-ray or neutron scattering (SAXS, SANS) in transmission allows for a determination of the interface width in a two phase system of a bulk sample (Porod law). Because of weak scattering this measurement is only possible with high scattering contrast between components and a strict two component system has to be assumed. An x-ray microbeam (0.05–20 μm in diameter) from a hard x-ray synchrotron source is used for so-called scanning x-ray microscopy where the beam is scanned over the sample to determine at each spot a full x-ray small or wide angle scattering pattern with an area detector. Structural information at micro- to nanometer level is obtained, spatially resolved at different locations of the sample.

4.10 Secondary Ion Mass Spectrometry (SIMS)

Secondary ion mass spectrometry (SIMS) may be used to determine the chemical composition of surfaces and interfaces at high resolution [3, 63, 65]. Secondary ions are generated by bombardment of the sample surface with an ion beam under vacuum. Those generated ions from the sample are analyzed in a mass spectrometer. The organic characteristic fragments are used for identification of the composition (fingerprint technique). In the “static” mode of operation at low ion flux, only a monolayer is removed from the surface (static SIMS). This mode is used for surface investigations and allows for instance very sensitive investigations of surface contaminations.

At high incident ion flux in the “dynamic” mode (Fig. 17), the sample material is continuously sputtered away, and by monitoring the secondary ion flux one generates a depth profile of elements and fragments (dynamic SIMS). At constant sputter rate also interfaces between polymers may be investigated, and depending on sputter rate a depth resolution as small as 12 nm may be achieved.

4.11 Ion Techniques

Several techniques use ions as probes for interface analysis besides SIMS (Figs. 16 and 17) [3]. They require dedicated equipment and are usually applied under ultra-high vacuum. Typically an ion accelerator in the appropriate energy range as well as corresponding ion sources and detectors are needed. Deuteration of one component is again a technique for contrast generation between polymers [54]. While the resolution is reasonably good, ion techniques are quite helpful for interface width determination of polymers. Elastic Recoil Detection/Forward Recoil Detection and Nuclear Reaction Analysis are typical and well-developed techniques. When heavy atoms are present in the sample, Rutherford Backscattering can be used.

A common lab technique uses scanning of a focused ion beam (FIB) for imaging, but in a cross beam set-up is often utilized in combination with a SEM for micro-/

nano-machining of a sample (cutting, milling, etching, ion deposition). The ion beam can etch deep cuts into the sample, which then are investigated by SEM or TEM further. In this way, hidden interfaces may be visualized, and the ion beam is also able to cut soft/hard interfaces, which otherwise may be difficult to achieve. Many possibilities for nano-machining, ion-beam lithography and nano-pattern generation exist, but one should be aware that after FIB treatment there is always a thin surface layer which contains some incident ions and has been modified by the ion beam. By FIB machining, structures may be generated down to the range of 10 nm. The combination of FIB and SEM in commercial instruments offers the possibility of simultaneous imaging of the treated region with the SEM at high resolution, while the ion beam is machining the surface. With added nano-manipulators for instance conductivity measurements can be performed. Various materials like Pt, W, SiO₂, etc. may be locally deposited on a sample surface in the FIB using ion-beam-activated deposition by local decomposition of molecules from a directed gas flow. The FIB in this way can be considered as a nano-lab.

4.12 Optical Microscopy Techniques (OM)

If nanoscopic resolution is not required, optical microscopy techniques provide easy possibilities of lateral imaging of the surface under atmospheric conditions and in some cases also at an interface of the sample. In standard operation, lateral resolution is limited by the wavelength of light, which ranges typically from 300 nm to micrometers. With a tiny waveguide, the lateral resolution can be enhanced to some nanometers (SNOM). Interference techniques improve the sampling depth, and it is enhanced for instance with phase measurement interference microscopy to 0.5 nm. Fluorescence techniques can also reach nanoscopic resolution. Several microscopic techniques are available at different level of sophistication to be used for surface and interface characterization:

Light microscopy in reflection or transmission mode with dark field or differential interference contrast for lateral inhomogeneities, Brewster-angle, ellipsometric, or surface plasmon microscopy for thickness determination, phase measurement interference microscopy for surface topography with subnanometer height resolution, fluorescence microscopy with labeled molecules for distribution and movement of molecules also at nanoscale, IR, or Raman microscopy for lateral distribution and identification of molecules, as well as confocal laser scanning microscopy for lateral and depth sensitivity in sub-micrometer range. The resolution limit of fluorescence microscopy has recently been significantly reduced by specific techniques, which allow for instance measurements of cells and bio-objects at resolution in the nano-range.

4.13 Indentation, Adhesion, Mechanical Properties

A classical mechanical surface characterization is the hardness determination [3]. A hardness measurement is done by indenting a well-defined diamond stylus at a

certain load into the surface measuring the depth of the indent. The test was miniaturized for the investigation of thin layers and anisotropic materials (micro-hardness test). Here a small diamond stylus of well-defined geometry is used, and both indentation depth and indentation load are simultaneously recorded as function of time. From an analysis of the load-displacement data, both the hardness and the Young's modulus can be calculated. Hardness as well as stiffness images of a surface are obtained by scanning the surface. With appropriate tips nano-indentation experiments are performed with a scanning force microscope. The surface can be deformed elastically, and knowing the cantilever stiffness a stiffness image of the surface is obtained. However, quantitative stiffness values are difficult to obtain and the technique is usually used only in a qualitative way to obtain a stiffness contrast between components for lateral imaging.

This is similarly performed for friction and adhesion of the tip at the surface and corresponding images are obtained. Here the adhesion of the cantilever tip to the surface is determined, but also colloidal particles may be attached to the cantilever for example. Tests of adhesion of films deposited on a surface are essentially fracture tests. Adhesion of those films is most commonly measured by peel tests, but may also be determined from blister or double cantilever beam tests. Adhesion tests should be performed in view of the desired application, since values depend in most cases on the measurement technique used. This is similarly true for friction between two solid samples, which can be measured at macroscopic and microscopic level utilizing different techniques and local probes. One should keep in mind that mechanical properties at the surface and interface can be very different from the bulk, and a detailed understanding is still missing.

4.14 Inverse Gas Chromatography (IGC)

From a measurement of the adsorption of test gases (and vapors of liquids) at surface of a material one can get interesting information on surface activity, composition, and phase transitions. While gas chromatography is aiming at the characterization of the adsorbing gas, inverse gas chromatography is aiming at the characterization of the surface of the filler material, which can be a polymer powder or fiber. Specific gases ("probes") of known properties are utilized to determine the interaction behavior, to provide surface characteristics and functionality of the filler material. A commercial gas chromatographic apparatus can be used, and the method is relatively cheap and easy to apply.

As mentioned before, we cannot cover details of the surface and interface characterization techniques because of the wealth of techniques used. In addition, there is fast technical development in many areas and resolution depends largely on experimental conditions and samples, which have to be prepared in a dedicated way to achieve optimal resolution or contrast. The conclusions given above therefore have to be taken with care. One always should keep in mind that the choice of a suitable and optimal technique for a particular problem is of crucial importance and should consider aspects like sample preparation, necessary spatial and depth resolution, contrast generation, as well as environmental conditions needed.

5 Summary and Outlook

Polymer surfaces and interfaces are important for nearly all polymer materials and determine many properties. In this chapter a short outline of polymer surfaces at molecular scale is given with reference to special aspects of chain conformation and surface dynamics. In this respect, the surface tension as a fundamental property of a surface is discussed. Surface functionalization can change appearance of a material very significantly. In particular, the grafting of polymer brushes onto surfaces is described as a very versatile tool, where even responsive polymer brush surfaces can be obtained and wetting, adhesion, bio-functionality, catalytic activity and sensing ability controlled. From the theoretical side, the interface between polymers can be formulated on the basis of mean-field theory with introduction of an effective interaction parameter, which is related with interface width and fluctuations at the interface. Examples are polymer blends, copolymers as compatibilizers and composites, where interfaces play an essential role. Important for surface and interface characterization are dedicated techniques, which include scanning force and electron microscopy, photoelectron and IR/Raman spectroscopy as well as x-ray and neutron reflectometry or scattering techniques. For their efficient use, guidelines for resolution and typical information obtained are provided.

Polymer surfaces and interfaces and the functionalization in their vicinity are becoming more and more important with the development of more complex and nanoscale devices and materials. So requirements for functional coating are getting more and more challenging, and self-cleaning, multifunctional, responsive or adaptive coatings are desired. Similarly nanocomposites with dedicated properties require particular functionalization of the surface of the nanoparticles for good dispersion and interfacial adhesion. In microelectronics industry the design of nanoscopic thin and structured multilayer films provides a challenge to interfacial design concerning adhesion, wetting, roughness, electron transport and optical as well as mechanical properties of polymers used for the design and fabrication of the nano-electronic devices. This becomes even more demanding with the introduction of flexible devices, where typically a flexible polymer film is used as a support. So there are plenty of problems and questions connected with surfaces and interfaces in the design of future advanced devices and materials. They require a good fundamental understanding of surface and interface properties, which is only possible with highly advanced characterization techniques. So this area will also in the future be under constant development.

References

1. I. C. Sanchez (ed.), *Physics of Polymer Surfaces and Interfaces* (Butterworth-Heinemann, Boston, 1992)
2. R.A.L. Jones, *Polymers at Surfaces and Interfaces* (Cambridge University Press, Cambridge, 2008)

3. M. Stamm (ed.), *Polymer Surfaces and Interfaces: Characterization, Modification and Application* (Springer, Berlin/Heidelberg, 2008)
4. G.J. Fleer, *Polymers at Interfaces* (Springer, Berlin, 2013)
5. A. Karim, S. Kumar, *Polymer Surfaces Interfaces and Thin Films* (World Scientific, Singapore, 1999)
6. A.N. Netravali, *Interface/Interphase in Polymer Nanocomposites* (Wiley Academic, New Jersey, 2017)
7. S. Fakirov (ed.), *Nano-size Polymers* (Springer International, Cham, 2016)
8. S. Wu, *Polymer Interface and Adhesion* (Marcel Dekker, New York, 1982)
9. J.N. Israelachvili, *Intermolecular and Surface Forces* (Academic Press, London, 1991)
10. K. Binder, Theories and mechanism of phase transitions, heterophase polymerizations, homopolymerization, addition polymerization. *Adv. Pol. Sci.* **112**, 181 (1994)
11. F. Kremer, W. Richtering (eds.), Characterization of polymer surfaces and thin films. *Progr. Colloid Polym. Sci.* **132**, 1–171 (2006)
12. J.-U. Sommer, M. Stamm, in *Surface and Interface Science*, ed. by K. Wandelt, vol. 1–8 (Wiley, 2019)
13. I.V. Gerasimchuk, J.-U. Sommer, Mean-field treatment of polymer chains trapped between surfaces and penetrable interfaces. *Phys. Rev. E* **76**, 041803, 1–11 (2007)
14. M. Stamm, J.-U. Sommer, Polymer–nanoparticle films: Entropy and enthalpy at play. *Nat. Mater.* **6**, 260–261 (2007)
15. P.G. de Gennes, Polymer solutions near interfaces. 1. Adsorption and depletion layers. *Macromolecules* **14**, 1637 (1981)
16. R. Descas, J.-U. Sommer, A. Blumen, Static and dynamic properties of tethered chains at adsorbing surfaces: A Monte Carlo study. *J. Chem. Phys.* **120**(18), 8831–8840 (2004)
17. G.-L. He, R. Messina, H. Löwen, A. Kiriy, V. Bocharova, M. Stamm, Shear-induced stretching of adsorbed polymer chains. *Soft Matter* **5**, 3014–3017 (2009)
18. S. Minko, A. Kiriy, G. Gorodyska, M. Stamm, Single flexible hydrophobic polyelectrolyte molecules adsorbed on solid substrate: Transition between stretched chain, necklace-like conformation and globule. *J. Am. Chem. Soc.* **124**, 3218–3219 (2002)
19. J. Kraus, P. Müller-Buschbaum, T. Kuhlmann, D.W. Schubert, M. Stamm, Confinement effects on the chain conformation in thin polymer films. *Europhys. Lett.* **49**, 210 (2000). J. Kraus, PhD thesis, Mainz (1999)
20. S.T. Wu, G.H. Fredrickson, J.-P. Carton, A. Ajdari, L. Leibler, Distribution of chain ends at the surface of a polymer melt: Compensation effects and surface tension. *J. Polym. Sci. B* **33**, 2373–2389 (1995)
21. J. Baschnagel, K. Binder, On the influence of hard walls on structural properties in polymer glass simulation. *Macromolecules* **28**, 6808–6818 (1995)
22. A. Galuschko, M. Lang, T. Kreer, J.-U. Sommer, Monte Carlo simulation of thin film polymer melts. *Soft Mater.* **12**, 49–55 (2014)
23. L. Si, M.V. Massa, K. Dalnoki-Veress, H.R. Brown, R.A.L. Jones, Chain entanglement in thin freestanding polymer films. *PRL* **94**, 127801 (2005)
24. R.S. PaiPanandiker, J.R. Dorgan, T. Pakula, Static properties of homopolymer melts in confined geometries determined by Monte Carlo simulation. *Macromolecules* **30**, 6348–6352 (1997)
25. M. Doi, S.F. Edwards, *The Theory of Polymer Dynamics* (Clarendon Press, Oxford, 1986)
26. P. Müller-Buschbaum, M. Stamm, Correlated roughness, long-range correlations and dewetting of thin polymer films. *Macromolecules* **31**, 3686–3692 (1998)
27. N. Rehse, C. Wang, M. Hund, M. Geoghegan, R. Magerle, G. Krausch, Stability of thin polymer films on a corrugated substrate. *Europ. Phys. E* **4**, 69–76 (2001)
28. M. Vlatkov, J.-L. Barrat, Local dynamics and primitive path analysis for a model polymer melt near a surface. *Macromolecules* **40**, 3797–3804 (2007)
29. J.A. Forrest, K. Dalnoki-Veress, J.R. Stevens, J.R. Dutcher, Effect of free surfaces on the glass transition temperature of thin polymer films. *PRL* **77**, 2002 (1996)

30. M. Erber, M. Tress, E.U. Mapesa, A. Serghei, K.-J. Eichhorn, B. Voit, F. Kremer, Glassy dynamics and glass transition in thin polymer layers of PMMA deposited on different substrates. *Macromolecules* **43**, 7729–7733 (2010)
31. T. Kuhlmann, J. Kraus, P. Müller-Buschbaum, D.W. Schubert, M. Stamm, Effects of confined geometry and substrate interaction on the initial stages of interdiffusion in thin polymer films. *J. Non-Cryst. Solids* **235–237**, 457 (1998)
32. A.W. Adamson, A.P. Gast, *Physical Chemistry of Surfaces* (Wiley, New York, 1997)
33. M. Daoud, C.E. Williams, *Soft Matter Physics* (Springer, Berlin, 1999)
34. S. Minko, M. Müller, M. Motornov, M. Nitschke, K. Grundke, M. Stamm, Two-level structured self-adaptive surfaces with reversibly tunable properties. *J. Am. Chem. Soc.* **125**, 3896–3900 (2003)
35. M.A. Cohen Stuart, W.T.S. Huck, J. Genzer, M. Müller, C. Ober, M. Stamm, G.B. Sukhorukov, I. Szleifer, V.V. Tsukruk, M. Urban, F. Winnik, S. Zauscher, I. Luzinov, S. Minko, Emerging applications of stimuli-responsive polymer materials. *Nat. Mater.* **9**, 101–113 (2010)
36. M. Krishnamoorthy, S. Hakobyan, M. Ramstedt, J.E. Gautrot, Surface-initiated polymer brushes in the biomedical field: Applications in membrane science, biosensing, cell culture, regenerative medicine and antibacterial coatings. *Chem. Rev.* **114**, 10976–11026 (2014)
37. L. Wu, J. Baghdachi, *Functional Polymer Coatings: Principles, Methods, and Applications* (Wiley, New York, 2015)
38. J. Rühe, M. Ballauff, M. Biesalski, P. Dzięzok, F. Gröhn, D. Johannsmann, N. Houbenov, N. Hugenberg, R. Konradi, S. Minko, M. Motornov, R.R. Netz, M. Schmidt, C. Seidel, M. Stamm, T. Stephan, D. Usov, H. Zhang, Polyelectrolyte brushes. *Adv. Polym. Sci.: Chem. Mater. Sci.* **165**, 79–150 (2004)
39. P. Mocny, H.A. Klok, Tribology of surface-grafted polymer brushes. *Mol. Syst. Design Eng.* **1**, 141–154 (2016)
40. A. Bousquet, H. Awada, R.C. Hiorns, Conjugated-polymer grafting on inorganic and organic substrates: A new trend in organic electronic material. *Prog. Polym. Sci.* **39**, 1847–1877 (2014)
41. E. Psarra, E. Foster, U. König, J. You, Y. Ueda, K.-J. Eichhorn, M. Müller, M. Stamm, A. Revzin, P. Uhlmann, Growth factor-bearing polymer brushes-versatile bioactive substrates influencing cell response. *Biomacromolecules* **11**, 3530–3542 (2015)
42. R.C. Advincula, W.J. Britain, K.C. Caster, in *Polymer Brushes*, ed. by J. Rühe (Wiley-VCH, Weinheim, 2004)
43. P. Uhlmann, H. Merlitz, J.-U. Sommer, M. Stamm, Polymer brushes for surface tuning. *Macromol. Rapid Commun.* **30**, 732–740 (2009)
44. S. Alexander, Polymer adsorption on small spheres: A scaling approach. *J. Phys. (Paris)* **38**, 977–982 (1977).; P.G. de Gennes, Conformation of polymers attached to an interface. *Macromolecules*, **13**, 1069–1075 (1980)
45. A. Halperin, M. Tirrell, T.P. Lodge, Tethered chains in polymer microstructures. *Adv. Polym. Sci.* **100**, 31–71 (1992)
46. W.J. Brittain, S. Minko, A structural definition of polymer brushes. *J. Polym. Sci., Part A: Polym. Chem.* **45**, 3505–3512 (2007)
47. L. Ionov, N. Houbenov, A. Sidorenko, M. Stamm, Inverse and reversible switching gradient surfaces from mixed polyelectrolyte brushes. *Langmuir* **20**, 9916–9919 (2004)
48. P. Uhlmann, L. Ionov, N. Houbenov, M. Nitschke, K. Grundke, M. Motornov, S. Minko, M. Stamm, Surface functionalization by smart coatings: Stimuli-responsive binary polymer brushes. *Prog. Org. Coat.* **55**, 168–174 (2006)
49. L. Ionov, S. Sapra, A. Synytska, A.L. Rogaci, M. Stamm, S. Diez, Fast and spatially resolved environmental probing using stimuli-responsive polymer layers and fluorescent nanocrystals. *Adv. Mater.* **18**, 1453–1457 (2006)
50. M. König, D. Magerl, M. Philipp, K.-J. Eichhorn, M. Müller, P. Müller-Buschbaum, M. Stamm, P. Uhlmann, Nanocomposit coatings with stimuli-responsive catalytic activity. *RSC Adv.* **4**, 17579–17586 (2014)
51. M. Stamm, D.W. Schubert, Interfaces between incompatible polymers. *Annu. Rev. Mater. Sci.* **25**, 325 (1995)

52. M. Stamm, Polymer surfaces, interfaces and thin films studied by x-ray and neutron reflectometry, in *Scattering in Polymeric and Colloidal Systems*, ed. by W. Brown, K. Mortensen (Gordon and Breach, Amsterdam, 2000), p. 495
53. L. Leibler, Theory of phase equilibria in mixtures of copolymers and homopolymers. *Macromolecules* **15**, 1283–1290 (1982)
54. R. Schnell, M. Stamm, The self-organisation of diblock copolymers at polymer blend interfaces. *Phys. B* **234**, 247 (1997).; R. Schnell, M. Stamm, F. Rauch, Segregation of diblock copolymers to the interface between weakly incompatible polymers. *Macromol. Chem. Phys.* **200**, 1806–1812 (1999)
55. I.W. Hamley, *The Physics of Block Copolymers* (Oxford University Press, Oxford, 1998)
56. E.B. Gowd, M.S. Rama, M. Stamm, Nanostructures based on self-assembly of block copolymers, in *Nanofabrication: Techniques and Principles*, ed. by M. Stepanova, S. Dew (Springer, Berlin, 2012), pp. 191–216
57. B. Nandan, M. Stamm, Self-assembled polymer supramolecules as templates for nanomaterials, in *Supramolecular Chemistry: From Molecules to Nanomaterials*, ed. by J. W. Steed, P. A. Gale, vol. 7 (Wiley, Chichester, 2012), pp. 3563–3586
58. A. Horechyy, B. Nandan, N.E. Zafeiropoulos, P. Formanek, U. Oertel, N.C. Bigall, A. Eychmüller, M. Stamm, A step-wise approach for dual nanoparticle patterning via block copolymer self-assembly. *Adv. Funct. Mater.* **23**, 483–490 (2013)
59. A. Sidorenko, I. Tokarev, S. Minko, M. Stamm, Ordered reactive nanomembranes/nanotemplates from thin films of block copolymer thin films supramolecular assembly. *J. Am. Chem. Soc.* **125**, 12211–12216 (2003)
60. B. Nandan, E.B. Gowd, N.C. Bigall, A. Eychmüller, P. Formanek, P. Simon, M. Stamm, Arrays of inorganic nanodots and nanowires using nanotemplates based on switchable block copolymer supramolecular assemblies. *Adv. Funct. Mater.* **19**, 2805–2811 (2009)
61. S. Sanwaria, A. Horechyy, D. Wolf, C.-Y. Chu, H.-L. Chen, P. Formanek, M. Stamm, R. Srivastava, B. Nandan, Helical packing of nanoparticles confined in cylindrical domains of a self-assembled block copolymer structure. *Angew. Chem. Int. Ed.* **53**(1–5), 9090 (2014)
62. G.J. Vancso, H. Schönherr, *Scanning Force Microscopy of Polymers* (Springer, Berlin, 2016)
63. L. Sabbatini (ed.), *Polymer Surface Characterization* (de Gruyter, Berlin, 2014)
64. G.H. Michler, *Electron Microscopy of Polymers* (Springer, Berlin, 2010)
65. D. Briggs, *Surface Analysis of Polymers by XPS and Static SIMS* (Cambridge University Press, Cambridge, 2009)
66. K. Hinrichs, D. Aulich, L. Ionov, N. Esser, K.-J. Eichhorn, M. Motornov, M. Stamm, S. Minko, Chemical and structural changes in a pH-responsive mixed polyelectrolyte brush studied by infrared Ellipsometry. *Langmuir* **25**, 10987–10991 (2009)
67. D.S. Fryer, P.F. Nealey, J.J. Pablo, Thermal probe measurements of the glass transition temperature for ultrathin polymer films as a function of thickness. *Macromolecules* **33**, 6439–6447 (2000)
68. P. Truman, P. Uhlmann, M. Stamm, Monitoring liquid transport and chemical composition in lab on a chip systems using ion sensitive FET devices. *Lab Chip* **6**, 1220–1228 (2006)
69. S. Gupta, M. Agrawal, M. Conrad, N.A. Hutter, P. Olk, F. Simon, L.M. Eng, M. Stamm, R. Jordan, Poly(2-(dimethylamino)ethyl methacrylate) brushes with incorporated nanoparticles as a SERS active sensing layer. *Adv. Funct. Mater.* **20**, 1756–1761 (2010)